14) Koizumi S, Saito Y, Nakazawa K, Nakajima K, Sawada J I, Kohsaka S, Illes P, and Inoue K : *Life Sci.* 72, 431-442, 2002
15) Cotrina ML, Lin JH, Alves-Rodrigues A, Liu S, Li J, Azmi-Ghadimi H, Kang J, Naus CC, and Nedergaard M. : *Proc. Natl. Acad. Sci. USA* 95, 15735-15740, 1998
16) Stout CE, Costantin JL, Naus CC, and Charles AC : *J. Biol. Chem.* 277, 10482-10488, 2002
17) Verderio C, and Matteoli M : *J. Immunol.* 166, 6383-6391, 2001
18) Schipke CG, Boucsein C, Ohlemeyer C, Kirchhoff F, and Kettenmann H. : *Faseb. J.* 16, 255-257, 2002
19) Cornell-Bell AH, Finkbeiner SM, Cooper MS, and Smith SJ. : *Science* 247, 470-473, 1990
20) Koizumi S, Fujishita K, Tsuda M, and Inoue K : *Drug Development Research* 59, 88-94, 2003
21) Rubio ME, and Soto F. : *J. Neurosci.* 21, 641-653, 2001
22) Moore D, Chambers J, Waldvogel H, Faull R, and Emson P. : *J. Comp. Neurol.* 421, 374-384, 2000
23) Bowser DN, Williams SR, and Khakh BS : *Society for Neuroscience Abstract* 251.5, 2003
24) Koizumi S, and Inoue K. : *Br. J. Pharmacol.* 122, 51-58, 1997
25) Koizumi S, Fujishita K, Tsuda M, Shigemoto-Mogami Y, and Inoue K. : *Proc. Natl. Acad. Sci. USA* 100, 11023-11028, 2003
26) Nett WJ, Oloff SH, and McCarthy KD. : *J. Neurophysiol.* 87, 528-537, 2002
27) Tsuda M, Shigemoto-Mogami Y, Koizumi S, Mizokoshi A, Kohsaka S, Salter M W, and Inoue K. : *Nature* 424, 778-783, 2003

小泉　修一（こいずみ・しゅういち）
国立医薬品食品衛生研究所 薬理部室長
1992 年九州大学大学院薬学研究科博士課程修了、（財）ヒューマンサイエンス振興財団博士研究員を経て、95 年厚生省入省。96 年英国ケンブリッジ大学 Babraham 研究所博士研究員。98 年帰国後、国立医薬食品衛生研究所主任研究官、2003 年より同室長。
専門分野は、中枢神経系薬理・生理。

GLIA 89:89–95 (2004)

Activation of p38 Mitogen-Activated Protein Kinase in Spinal Hyperactive Microglia Contributes to Pain Hypersensitivity Following Peripheral Nerve Injury

MAKOTO TSUDA,[1] AKITO MIZOKOSHI,[2] YUKARI SHIGEMOTO-MOGAMI,[1] SCHUICHI KOIZUMI,[3] AND KAZUHIDE INOUE[1,2]*

[1]*Division of Biosignaling, National Institute of Health Sciences, Tokyo, Japan*
[2]*Department of Molecular and System Pharmacology, Graduate School of Pharmaceutical Sciences, Kyushu University, Higashi, Fukuoka, Japan*
[3]*Division of Pharmacology, National Institute of Health Sciences, Tokyo, Japan*

KEY WORDS mitogen-activated protein kinases; dorsal horn; tactile allodynia; neuropathic pain

ABSTRACT Neuropathic pain is an expression of pathological operation of the nervous system, which commonly results from nerve injury and is characterized by pain hypersensitivity to innocuous stimuli, a phenomenon known as tactile allodynia. The mechanisms by which nerve injury creates tactile allodynia have remained largely unknown. We report that the development of tactile allodynia following nerve injury requires activation of p38 mitogen-activated protein kinase (p38MAPK), a member of the MAPK family, in spinal microglia. We found that immunofluorescence and protein levels of the dually phosphorylated active form of p38MAPK (phospho-p38MAPK) were increased in the dorsal horn ipsilateral to spinal nerve injury. Interestingly, the phospho-p38MAPK immunofluorescence in the dorsal horn was found exclusively in microglia, but not in neurons or astrocytes. The level of phospho-p38MAPK immunofluorescence in individual microglial cells was much higher in the hyperactive phenotype in the ipsilateral dorsal horn than the resting one in the contralateral side. Intrathecal administration of the p38MAPK inhibitor, 4-(4-fluorophenyl)-2-(4-methylsulfonylphenyl)-5-(4-pyridyl)-1H-imidazole (SB203580), suppresses development of the nerve injury-induced tactile allodynia. Taken together, our results demonstrate that nerve injury-induced pain hypersensitivity depends on activation of the p38MAPK signaling pathway in hyperactive microglia in the dorsal horn following peripheral nerve injury.

INTRODUCTION

Nerve injury arising from disease or physical trauma produces long-lasting abnormal hypersensitivity to innocuous stimuli, a phenomenon known as tactile allodynia (Woolf and Mannion, 1999; Scholz and Woolf, 2002). Tactile allodynia is a hallmark, and the most troublesome, of neuropathic pain syndrome in humans. It is nearly always resistant to known treatments such as nonsteroidal antiinflammatory agents (NSAIDs) or even narcotics (Woolf and Mannion, 1999; Scholz and Woolf, 2002). The mechanisms by which nerve injury develops tactile allodynia have remained largely unknown. It is thus essential to identify the molecular changes that lead to tactile allodynia in an effort to both understand its mechanisms and develop new therapies.

Makoto Tsuda is currently at the Programme in Brain and Behaviour, Hospital for Sick Children, 555 University Avenue, Toronto, Ontario M5G 1X8, Canada.

Grant sponsor: Uehara Memorial Foundation; Grant sponsor: Organization for Pharmaceutical Safety and Research; Grant sponsor: Ministry of Education, Science, Sports, and Culture of Japan; Grant sponsor: Japan Health Sciences Foundation.

*Correspondence to: Kazuhide Inoue, Division of Biosignaling, National Institute of Health Sciences, 1-18-1 Kamiyoga, Setagaya-ku, Tokyo 158-8501, Japan. E-mail: inoue@nihs.go.jp

Received 11 April 2003; Accepted 1 July 2003

DOI 10.1002/glia.10308

Several lines of evidence have proposed that induction of tactile allodynia is attributed to central hyperactive states resulting from multiple plastic alterations in dorsal horn neurons as well as glia following nerve injury (Woolf and Mannion, 1999; Woolf and Salter, 2000; Watkins et al., 2001; Scholz and Woolf, 2002). Recent models of nerve injury-induced plasticity in the dorsal horn postulate that induction of the spinal plasticity requires activation of intracellular signaling events including protein kinases for transcriptional and posttranscriptional modifications of various proteins such as cell surface receptors (Woolf and Salter, 2000). It is thus expected that protein kinases, including protein kinase Cγ (Malmberg et al., 1997), in the dorsal horn must regulate nerve injury-induced tactile allodynia; however, their remains poorly understood.

We report that development of tactile allodynia following nerve injury depends on p38 mitogen-activated protein kinase (p38MAPK), one of four subgroups of the MAPK family (Ono and Han, 2000); activation of p38MAPK is found in hyperactive microglia, but not in neurons or astrocytes in the dorsal horn after nerve injury. Thus, the present study suggests that p38MAPK in spinal microglia is an essential intracellular protein kinase that regulates pain hypersensitivity following peripheral nerve injury. Preliminary results of this study have been reported in abstract form (Tsuda et al., 2002a,b).

MATERIALS AND METHODS

Animals

Male Wistar rats were used in this study: rats weighing 200–230 g for the biochemical and immunohistochemical experiments, and rats weighing 270–290 g for the behavioral experiments testing the effect of intrathecal treatment with a p38MAPK inhibitor. We have confirmed that p38MAPK phosphorylation in the dorsal horn following nerve injury is also observed in both weight ranges of rats (data not illustrated). Rats were housed at a temperature of 22 ± 1°C with a 12-h light/dark cycle (light on 8:30 to 20:30) and were fed food and water ad libitum. All the animals used in the present study have been treated in accordance with the guidelines of National Institute of Health Sciences.

Neuropathic Pain Model

We used the spinal nerve injury model (Kim and Chung, 1992) with some modifications. A unilateral L5 spinal nerve of rats was tightly ligated and cut just distal to the ligature under isoflurane (2%) anesthesia. To assess the tactile allodynia, the calibrated von Frey filaments (0.4–15.1 g; Stoelting, Wood Dale, IL) were applied to the plantar surface of the hindpaw from below the mesh floor. The 50% paw withdrawal threshold was determined by the up-down method (Dixon, 1980; Chaplan et al., 1994).

Immunohistochemistry

The rats were deeply anesthetized by pentobarbital (100 mg/kg, i.p.) and perfused transcardially with 150 ml of phosphate-buffered saline (PBS; composition in mM: NaCl 137, KCl 2.7, KH_2PO_4 1.5, NaH_2PO_4 8.1; pH 7.4), followed by 300 ml of ice-cold 4% paraformaldehyde. The L5 segment of the lumbar spinal cord was removed, postfixed in the same fixative, and placed in 30% sucrose solution for 24 h at 4°C. Transverse L5 spinal cord sections (30 μm) were incubated in a blocking solution (3% normal goat serum [NGS]) and then incubated for 48 h at 4°C in the primary antibody, anti-phospho-p38MAPK (1:200; Cell Signaling, Beverly, MA). Markers of microglia, OX42 (anti-OX42, 1:100, Chemicon, Temecula, CA); astrocytes, glial fibrillary acidic protein (GFAP; anti-GFAP, 1:500; Boehringer-Mannheim, Indianapolis, IN); and neurons, NeuN (anti-NeuN, 1:200; Chemicon) were used to identify the type of phospho-p38MAPK-positive cells. Following incubation, tissue sections were washed and incubated for 3 h at room temperature in the secondary antibody solution (anti-rabbit IgG-conjugated Alexa Fluor™ 488 or anti-mouse IgG-conjugated Alexa Fluor 546, 1:1,000; Molecular Probes, Eugene, OR). The spinal cord sections were analyzed using a MicroRadiance Confocal Imaging System (Bio-Rad, Hercules, CA) and an Olympus IX70 microscope (Olympus Optical, Tokyo, Japan) equipped for epifluorescence. For quantitative assessment of the immunofluorescence staining of cells, we randomly selected dorsal horn fields displayed at high magnification. Microglia, as identified by OX42 immunofluorescence, were outlined; the immunofluorescence intensity of the phospho-p38MAPK was determined as the average pixel intensity within each cell. Background fluorescence intensity was determined and was subtracted from the value obtained for microglia.

Western Blotting

The rats were deeply anesthetized with pentobarbital (100 mg/kg, i.p.). The lumbar and sacral spinal cord was quickly removed and placed on a dish with ice-cold PBS. We identified the cord from L4 to L6 by the entry area of the dorsal roots and the shape of the cord under a microscope and cut at the boundary between L3 and L4 and between L6 and S1. The spinal cord segments L4-L6 ipsilateral to the nerve injury were homogenized in ice-cold PBS containing a mixture of phosphatase inhibitors (Sigma-RBI, St. Louis, MO) and protease inhibitors (Calbiochem, San Diego, CA). The homogenates were incubated with DNase and were sonicated. The resulting homogenate (20 μg) was subjected to 12.5% sodium dodecyl sulfate-polyacrylamide gel electrophoresis (SDS-PAGE), and the proteins were transferred electrophoretically to nitrocellulose membranes. After blocking, the membranes were incubated with anti-phospho-p38MAPK antibody (1:1,000; Cell Signal-

ing) or anti-p38MAPK antibody (1:1,000; Cell Signaling) and then were incubated with horseradish peroxidase (HRP)-conjugated secondary antibody. The blots were detected with a chemiluminescence method (LumiGLO; Cell Signaling) and exposed to autoradiography films (Hyperfilm-ECL; Amersham, Arlington Heights, IL).

Spinal Administration of p38MAPK Inhibitor

Under isoflurane (2%) anesthesia, rats were implanted with catheters for intrathecal injection according to the method described previously (Yaksh et al., 1980). A polyethylene tube (PE-10; 7.5 cm) was inserted through the atlanto-occipital membrane and to the lumbar enlargement (close to L4-L5 segments) and externalized through the skin. Rats were injected intrathecally with 4-(4-fluorophenyl)-2-(4-methylsulfonylphenyl)-5-(4-pyridyl)-1H-imidazole (SB203580; 30 nmol/10 μl) (Sigma-RBI) or vehicle [2% dimethylsulfoxide (DMSO)/10 μl] using a 25-μl Hamilton syringe with 28-gauge needle. Intrathecal injection of SB203580 or vehicle was started immediately after nerve injury (day 0) and given once a day for 14 days. SB203580 was dissolved in 100% DMSO and diluted by PBS (final concentration of DMSO: 2%). Behavioral testing was done 12–14 h after the injection of SB203580.

Statistical Analysis

Statistical analyses of the results were evaluated using the Student's *t*-test, the Student's paired *t*-test or the Mann-Whitney U-test.

RESULTS

p38MAPK Is Activated Exclusively in Hyperactive Microglia in the Dorsal Horn Following Peripheral Nerve Injury

Animals with L5 spinal nerve injury displayed tactile allodynia; the withdrawal threshold of the hindpaw, ipsilateral to nerve injury, to mechanical stimulation decreased progressively from 15.1 ± 0.1 g before the injury (day 0) to 3.0 ± 0.5 g at day 7 and to 2.1 ± 0.4 g (n = 7) at day 14 ($P < 0.001$, significantly different from the threshold on day 0) (Fig. 1A). In contrast, paw withdrawal threshold of the contralateral hindpaw was not changed significantly by nerve injury (Fig. 1A). To examine whether p38MAPK is activated in the dorsal horn of the spinal cord in rats that have developed tactile allodynia, we carried out immunofluorescence analysis with an antibody targeting the dually phosphorylated p38MAPK (phospho-p38MAPK), because p38MAPK members have a Thr-Gly-Tyr dual phosphorylation motif, requiring phosphorylation for its activation (Ono and Han, 2000). In L5 dorsal spinal cord

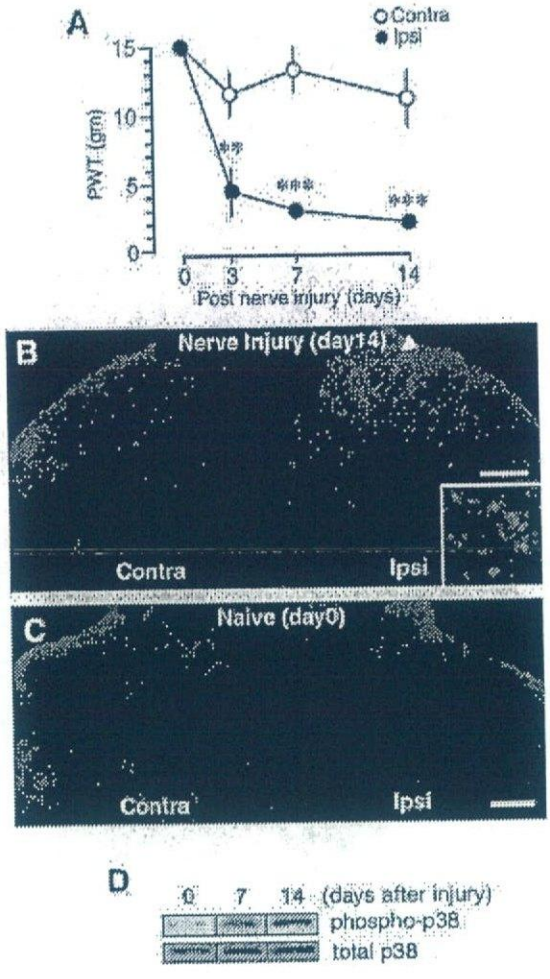

Fig. 1. p38 mitogen-activated protein kinase (p38MAPK) is dramatically activated in the spinal dorsal horn following L5 spinal nerve injury. **A:** The withdrawal threshold of tactile stimulation to the ipsilateral and contralateral hindpaw (PWT) was examined before nerve injury, 3, 7, and 14 days after nerve injury. Each data point represents the mean ±SEM of paw withdrawal threshold (in grams) (**$P < 0.01$, ***$P < 0.001$ by Student's paired *t*-test, compared with the threshold on day 0, n = 7). **B,C:** Immunoreactivity of phospho-p38MAPK (green) detected by an antibody for dual-phosphorylated p38MAPK in L5 dorsal spinal cord 14 days after nerve injury (B) and in that of naive rat (C) was visualized by immunofluorescence analysis using confocal microscopy. Highly magnified picture of the area (arrowhead) in B, shown in inset of B. **D:** Total protein from the spinal cord ipsilateral to the nerve injury on days 0 (naive), 7, and 14 was subjected to Western blot analysis. The proteins of phospho-p38MAPK and total p38MAPK were detected by an antibody for dual-phosphorylated and nonphosphorylated p38MAPK, respectively. Scale bars = 200 μm in B,C.

sections, at 14 days after nerve injury, we observed strong and punctate phospho-p38MAPK immunofluorescence on the ipsilateral side (Fig. 1B). The punctate labeling observed at low magnification was due to immunofluorescence of individual small cells, as shown under highly magnification (Fig. 1B, inset). In contrast, phospho-p38MAPK immunofluorescence was weaker and much less extensive in the dorsal horn contralat-

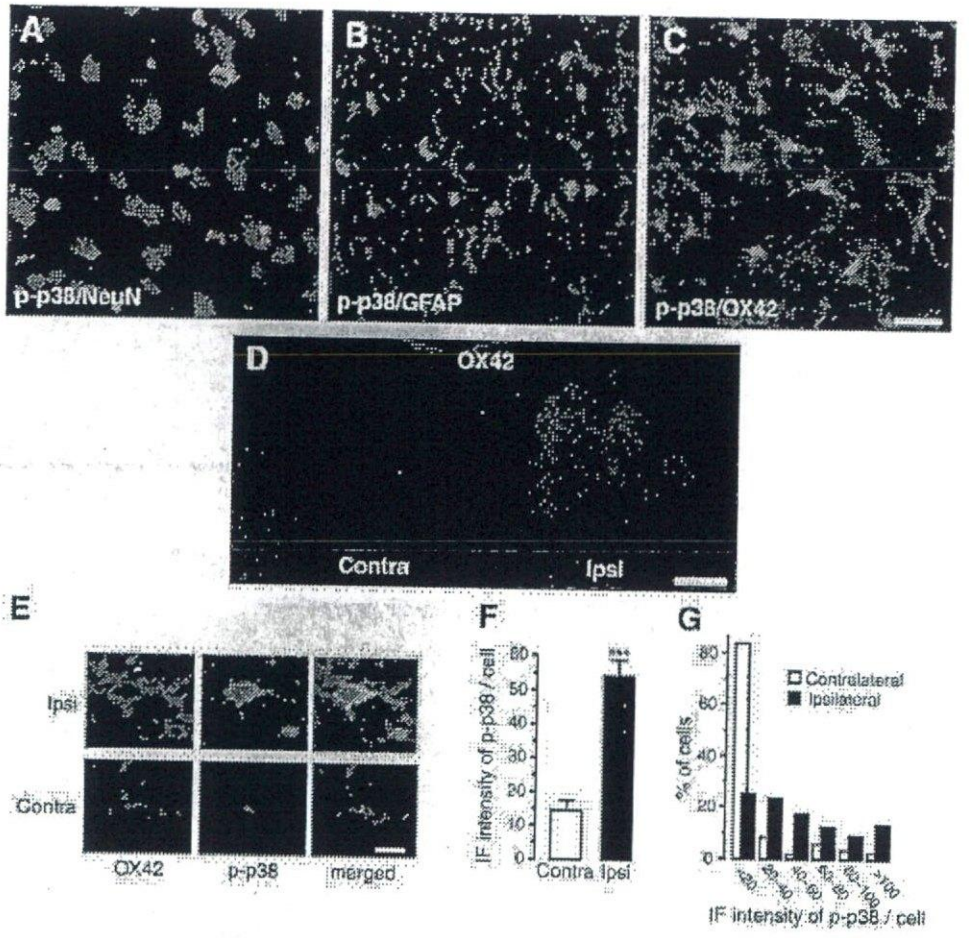

Fig. 2. p38 mitogen-activated protein kinase (p38MAPK) is activated in individual hyperactive microglia, but not in neurons or astrocytes in the dorsal horn following L5 spinal nerve injury. Immunostaining was carried out in L5 dorsal spinal cord sections at 14 days after nerve injury, using confocal microscopy. **A–C:** Double immunofluorescent labels of phospho-p38MAPK (green) with NeuN (A, red), a marker of neurons, glial fibrillary acidic protein (GFAP) (B, red), a marker of astrocytes, and OX42 (C, red), a marker of microglia, were analyzed. **D:** The change of the level of OX42 immunofluorescence (red) following nerve injury was examined in transverse section of L5 dorsal horn at 14 days after nerve injury. **E:** The different activation of p38MAPK in ipsilateral (Ipsi, top three panels) and contralateral (Contra, bottom three panels) microglia was examined. OX42, phospho-p38MAPK (p-p38) and merged immunofluorescences are shown in red, green, and yellow, respectively. **F:** Immunofluorescence intensity of phospho-p38MAPK in individual microglia was determined as the average pixel density in the ipsilateral (Ipsi; n = 83 OX42-positive cells) and contralateral (Contra; n = 74 OX42-positive cells) dorsal horn. Each data point represents the mean ±SEM of immunofluorescence (IF) intensity of phospho-p38MAPK (p-p38) per cell (***$P < 0.001$ by the Mann-Whitney U-test, compared with the value of contralateral dorsal horn). **G:** Histogram of the percentage of dorsal horn microglia displaying ranges of IF intensity values of phospho-p38MAPK in individual microglia. Ipsi, ipsilateral; Contra, contralateral. Scale bars = 25 μm in C; 200 μm in D; 10 μm in E.

eral to the nerve injury (Fig. 1B) or in that of naive rats (Fig. 1C). We further examined the level of phosphorylated p38MAPK protein in homogenates from the spinal cords of naive and nerve-injured rats by Western blot analysis; we found that the band intensity of phospho-p38MAPK protein in the ipsilateral spinal cord increased dramatically 7 and 14 days after nerve injury compared with that in naive rat (day 0) (Fig. 1D). The bilateral difference in phospho-p38MAPK levels parallels the emergence of the tactile allodynia (Fig. 1A). These results indicate that the p38MAPK is activated in the dorsal horn ipsilateral to the nerve injury, which may correlate with the nerve injury-induced tactile allodynia.

To identify the type of cell in which p38MAPK was phosphorylated after nerve injury, we carried out double immunolabeling for phospho-p38MAPK and for cell type-specific markers: for neurons, NeuN; for astrocytes, GFAP; or for microglia, OX42 (Honore et al., 2000). We found that cells showing phospho-p38MAPK immunofluorescence were not double-labeled for NeuN (0%, calculated in 110 cells, representative shown in Fig. 2A) or GFAP (0%, calculated in 132 cells, representative shown in Fig. 2B). Rather, almost all phospho-p38MAPK-positive cells (99%, calculated in 187 cells) were double-labeled with OX42 (representative shown in Fig. 2C), indicating that activation of p38MAPK in the dorsal horn is highly restricted to

microglia, but not found in neurons or astrocytes. OX42 recognizes the complement receptor type 3 (CR3), expression of which is greatly increased in hyperactive versus resting microglia (Aldskogius and Kozlova, 1998). We found that OX42 labeling was greater in the dorsal horn ipsilateral to the nerve injury (Fig. 2D), whereas OX42 labeling in the dorsal horn was low bilaterally in sham-operated animals (not illustrated). OX42-positive cells were more numerous (Fig. 2D) and displayed hypertrophic morphology (Fig. 2E) in the dorsal horn on the side of the nerve injury as compared with the contralateral side (Fig. 2D,E). These results indicate that nerve injury induced a switch from the resting to the hyperactive phenotype in the population of microglia in the dorsal horn. The cells labeled intensely with OX42 showed high levels of phospho-p38MAPK immunofluorescence (Fig. 2E, top panels). In contrast, resting microglia that showed a low level of OX42 had no or weak phospho-p38MAPK immunofluorescence (Fig. 2E, bottom panels). The mean level of intensity of phospho-p38MAPK immunofluorescence per OX42-positive cell was on average 3.7-fold higher in the ipsilateral (n = 83 cells) as compared with the contralateral dorsal horn (n = 74 cells) ($P < 0.001$; Fig. 2F). The distribution of phospho-p38MAPK immunofluorescence intensities per OX42-positive cell was skewed to the right (Fig. 2G). We conclude that, in the dorsal horn following nerve injury, hyperactive microglia are the cell type in which p38MAPK is activated and that the level of p38MAPK phosphorylation is dramatically increased in individual microglia. As shown in Figure 2E, subcellular distribution between phospho-p38MAPK and OX42 immunofluorescence is different, but our confocal microscopic Z-series analyses demonstrated that phospho-p38MAPK signals were found in the inside of OX42 signals which is known to localize on the cell surface (data not illustrated).

p38MAPK Activation in the Spinal Cord Is Required for Development of Tactile Allodynia Following Peripheral Nerve Injury

We examined whether intrathecal treatment with a potent inhibitor of p38MAPK, SB203580, through a catheter whose tip was positioned near the L4-L5 dorsal horn alters the development of tactile allodynia following nerve injury. Catheterized rats were treated with vehicle (2% DMSO/10 μl, n = 7) or SB203580 (30 nmol/10 μl, n = 9) once a day for 14 days, beginning on the day of the nerve injury. Intrathecal vehicle-treated rats displayed a marked decrease in paw withdrawal threshold following nerve injury ($P < 0.01$, significantly different from the threshold on day 0) (Fig. 3). In contrast, intrathecal SB203580-treated rats showed only a slight decrease in paw withdrawal threshold; paw withdrawal thresholds was not significantly decreased except for day 3 ($P < 0.01$, significantly different from the threshold on day 0). Paw withdrawal thresholds on day 7 and 14 were significantly greater in animals treated with SB203580 (n = 9) as compared with that in animals treated with vehicle (n = 7) (day 7: $P < 0.01$, day 14: $P < 0.001$, significantly different from the threshold of vehicle-treated group on days 7 and 14, respectively) (Fig. 3). These results suggest that intrathecal treatment with an inhibitor for p38MAPK in the spinal cord, the distribution of which is highly restricted in microglia, suppresses the development of tactile allodynia following spinal nerve injury.

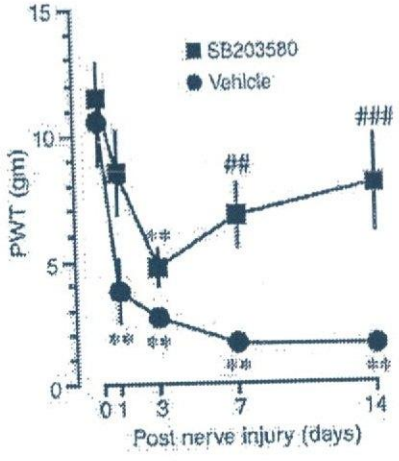

Fig. 3. Intrathecal administration of a potent inhibitor for p38 mitogen-activated protein kinase (p38MAPK), SB203580, suppresses development of tactile allodynia caused by L5 spinal nerve injury. Rats were injected intrathecally with SB203580 (30 nmol/10 μl, n = 9) or vehicle (2% dimethylsulfoxide [DMSO]/10 μl, n = 7) once a day for 14 days. The withdrawal threshold of tactile stimulation to the ipsilateral hindpaw (PWT) was examined on days 0 (before nerve injury), 1, 3, 7, and 14 at 12–14 h after intrathecal injection. Each data point represents the mean ±SEM of paw withdrawal threshold (in grams). $^{**}P < 0.01$ by the Student's paired t-test, compared with threshold on day 0; $^{\#\#}P < 0.01$; $^{\#\#\#}P < 0.001$, by the Mann-Whitney U-test, compared with the threshold of vehicle-treated group.

DISCUSSION

Our principal conclusion from the present findings is that following spinal nerve injury p38MAPK is activated in individual hyperactive microglia in the dorsal horn, leading to the development of nerve injury-induced pain hypersensitivity tactile allodynia, a major functional consequence of peripheral nerve injury. p38MAPK is the first intracellular signaling event, activation of which occurs exclusively in microglia, that regulates pain hypersensitivity caused by nerve injury. We showed a marked increase in immunofluorescence and protein levels of dual-phosphorylated p38MAPK in the dorsal horn after spinal nerve injury. These results are supported by previous findings that phosphorylation of p38MAPK is increased in response to the damage of the sciatic nerve or dorsal root (Murashov et al., 2001; Nomura et al., 2001; Kim et al., 2002) that projects to the dorsal spinal cord. p38MAPK has been

reported to be expressed in a number of cell types in the CNS in vivo (Lee et al., 2000; Maruyama et al., 2000). We found that in the neuropathic pain state, p38MAPK activation in the dorsal horn was not observed in neurons or astrocytes but, rather, occurred exclusively in microglia. As shown previously (Aldskogius and Kozlova, 1998), the number of microglia increased in the dorsal horn on the side of the nerve injury following nerve injury. We have recently demonstrated that the number of microglia is on average 2.2-fold greater in the ipsilateral side of the dorsal horn than in the contralateral side (Tsuda et al., 2003). We also show that marked phosphorylation of p38MAPK is observed in individual microglia in the ipsilateral dorsal horn (3.7-fold, as compared with the contralateral side), particularly in hyperactive microglia that dramatically expressed complement receptor type 3 recognized by OX42, and displayed hypertrophic morphology. The increase is more striking than the increase in the number of microglia in the ipsilateral side of the dorsal horn. Therefore, in the dorsal horn, following nerve injury, hyperactive microglia are the cell type in which p38MAPK is activated; in addition to an increase in the number of cells, the increased p38MAPK phosphorylation in individual hyperactive microglia would be one of the major components of p38MAPK activation in the dorsal horn following nerve injury. Moreover, we show that intrathecal treatment with SB203580, which binds to the ATP pocket in p38MAPK, and consequently inhibits its enzymatic activity (Tong et al., 1997), led to a statistically significant suppression of tactile allodynia on days 7 and 14 after nerve injury when the increase in p38MAPK phosphorylation was found. It appears that the suppression of tactile allodynia by SB203580 might be related to its inhibitory effect on the increased p38MAPK activity in the dorsal horn after nerve injury, based on the observations that intrathecal administration of SB203580 has no effect on basal pain responses in naive rats, which have a very low level of p38MAPK phosphorylation (Watkins et al., 1997; Murashov et al., 2001; Nomura et al., 2001; Ji et al., 2002; present data). Taking these results together, we conclude that development of tactile allodynia following nerve injury depends on activation of the p38MAPK signaling pathway in hyperactive microglia in the dorsal horn, although we cannot exclude the possible involvement of p38MAPK in DRG neurons (Kim et al., 2002).

p38MAPK activation in microglia is quite different from that of other MAPKs, extracellular signal-regulated kinases (ERK) and c-jun N-terminal or stress-activated protein kinases (JNK/SPAK), activation of which is found in dorsal horn astrocytes, but not in microglia, after peripheral nerve injury (Ma and Quirion, 2002). Thus, microglial regulation of tactile allodynia may require activation of p38MAPK, but not other MAPKs. Several extracellular substances have been reported to trigger p38MAPK activation in microglia in vitro, thereby regulating microglial functions (Koistinaho and Koistinaho, 2002). Tikka et al. (2001) have shown that glutamate-evoked proliferation of microglia and interleukin-1β (IL-1β) and nitric oxide release from microglia in the spinal cord primary culture depend on its p38MAPK activation. We have recently demonstrated that extracellular ATP activates p38MAPK in cultured microglia, thereby releasing tumor necrosis factor-α (TNF-α) and IL-6 (Hide et al., 2000; Shigemoto-Mogami et al., 2001). These cytokines are increased in the spinal cord following spinal nerve injury (Sweitzer et al., 2001; Winkelstein et al., 2001) and are involved in induction of nerve injury-induced tactile allodynia (Ramer et al., 1998; Sommer et al., 1998; Sweitzer et al., 2001). Therefore, elucidating p38MAPK activity-dependent microglial outputs, including the production of these cytokines in the dorsal horn in vivo, would help in understanding the mechanisms underlying the induction of pain hypersensitivity following nerve injury.

Nerve injury and peripheral inflammation that produce neuropathic and inflammatory pain states, respectively, have been known to induce distinct sets of neurochemical changes in the dorsal horn (Honore et al., 2000). In contrast to the present findings with peripheral nerve injury, Ji et al. (2002) have shown that p38MAPK activation does not occur in the dorsal horn under a sustained inflammation by intraplantar injection of complete Freund's adjuvant, which produces prolonged hypersensitivity to pain. Thus, p38MAPK activation in dorsal horn microglia would be a unique intracellular change following nerve injury, contributing to the development of nerve injury-induced pain hypersensitivity. This approach may provide a new therapeutic strategy specially targeting neuropathic pain. Importantly, in naive animals, p38MAPK activation is very weak in the dorsal horn (Fig. 1), and basal pain sensitivity is not affected by spinal administration of p38MAPK inhibitors (Watkins et al., 1997; Ji et al., 2002). This suggests a therapeutic benefit of interfering with p38MAPK activation in the treatment of neuropathic pain, without affecting normal pain sensitivity.

ACKNOWLEDGMENTS

The authors thank Michael W. Salter for critical comments on the manuscript, and Janice Hicks and Conor J. Gallagher for corrections of the manuscript. We thank Hideaki Obata, Masayuki Sasaki, Keiji Ishizaki, and Fumio Goto for advice on methods of intrathecal catheterization and L5 spinal nerve injury.

REFERENCES

Aldskogius H, Kozlova EN. 1998. Central neuron-glial and glial-glial interactions following axon injury. Prog Neurobiol 55:1–26.

Chaplan SR, Bach FW, Pogrel JW, Chung JM, Yaksh TL. 1994. Quantitative assessment of tactile allodynia in the rat paw. J Neurosci Methods 53:55–63.

Dixon WJ. 1980. Efficient analysis of experimental observations. Annu Rev Pharmacol Toxicol 20:441–462.
Hide I, Tanaka M, Inoue A, Nakajima K, Kohsaka S, Inoue K, Nakata Y. 2000. Extracellular ATP triggers tumor necrosis factor-alpha release from rat microglia. J Neurochem 75:965–972.
Honore P, Rogers SD, Schwei MJ, Salak-Johnson JL, Luger NM, Sabino MC, Clohisy DR, Mantyh PW. 2000. Murine models of inflammatory, neuropathic and cancer pain each generates a unique set of neurochemical changes in the spinal cord and sensory neurons. Neuroscience 98:585–598.
Ji RR, Samad TA, Jin SX, Schmoll R, Woolf CJ. 2002. p38 MAPK activation by NGF in primary sensory neurons after inflammation increases TRPV1 levels and maintains heat hyperalgesia. Neuron 36:57–68.
Kim SH, Chung JM. 1992. An experimental model for peripheral neuropathy produced by segmental spinal nerve ligation in the rat. Pain 50:355–363.
Kim SY, Bae JC, Kim JY, Lee HL, Lee KM, Kim DS, Cho HJ. 2002. Activation of p38 MAP kinase in the rat dorsal root ganglia and spinal cord following peripheral inflammation and nerve injury. NeuroReport 13:2483–2486.
Koistinaho M, Koistinaho J. 2002. Role of p38 and p44/42 mitogen-activated protein kinases in microglia. Glia 40:175–183.
Lee SH, Park J, Che Y, Han PL, Lee JK. 2000. Constitutive activity and differential localization of p38alpha and p38beta MAPKs in adult mouse brain. J Neurosci Res 60:623–631.
Ma W, Quirion R. 2002. Partial sciatic nerve ligation induces increase in the phosphorylation of extracellular signal-regulated kinase (ERK) and c-Jun N-terminal kinase (JNK) in astrocytes in the lumbar spinal dorsal horn and the gracile nucleus. Pain 99:175–184.
Malmberg AB, Chen C, Tonegawa S, Basbaum AI. 1997. Preserved acute pain and reduced neuropathic pain in mice lacking PKCγ. Science 278:279–283.
Maruyama M, Sudo T, Kasuya Y, Shiga T, Hu B, Osada H. 2000. Immunolocalization of p38 MAP kinase in mouse brain. Brain Res 887:350–358.
Murashov AK, Ul Haq I, Hill C, Park E, Smith M, Wang X, Goldberg DJ, Wolgemuth DJ. 2001. Crosstalk between p38, Hsp25 and Akt in spinal motor neurons after sciatic nerve injury. Brain Res Mol Brain Res 93:199–206.
Nomura H, Furuta A, Suzuki SO, Iwaki T. 2001. Dorsal horn lesion resulting from spinal root avulsion leads to the accumulation of stress-responsive proteins. Brain Res 893:84–94.
Ono K, Han J. 2000. The p38 signal transduction pathway: activation and function. Cell Signal 12:1–13.
Ramer MS, Murphy PG, Richardson PM, Bisby MA. 1998. Spinal nerve lesion-induced mechanoallodynia and adrenergic sprouting in sensory ganglia are attenuated in interleukin-6 knockout mice. Pain 78:115–121.
Scholz J, Woolf CJ. 2002. Can we conquer pain? Nat Neurosci 5(suppl):1062–1067.
Shigemoto-Mogami Y, Koizumi S, Tsuda M, Ohsawa K, Kohsaka S, Inoue K. 2001. Mechanisms underlying extracellular ATP-evoked interleukin-6 release in mouse microglial cell line, MG-5. J Neurochem 78:1339–1349.
Sommer C, Schmidt C, George A. 1998. Hyperalgesia in experimental neuropathy is dependent on the TNF receptor 1. Exp Neurol 151: 138–142.
Sweitzer S, Martin D, DeLeo JA. 2001. Intrathecal interleukin-1 receptor antagonist in combination with soluble tumor necrosis factor receptor exhibits an anti-allodynic action in a rat model of neuropathic pain. Neuroscience 103:529–539.
Tikka T, Fiebich BL, Goldsteins G, Keinanen R, Koistinaho J. 2001. Minocycline, a tetracycline derivative, is neuroprotective against excitotoxicity by inhibiting activation and proliferation of microglia. J Neurosci 21:2580–2588.
Tong L, Pav S, White DM, Rogers S, Crane KM, Cywin CL, Brown ML, Pargellis CA. 1997. A highly specific inhibitor of human p38 MAP kinase binds in the ATP pocket. Nat Struct Biol 4:311–316.
Tsuda M, Mizokoshi A, Shigemoto-Mogami Y, Koizumi S, Inoue K. 2002a. p38 mitogen-activated protein kinase (p38MAPK) is activated in the spinal microglia of neuropathic pain model. Jpn J Pharmacol 88:82.
Tsuda M, Mizokoshi A, Mogami Y, Koizumi S, Inoue K. 2002b. Activation of p38 mitogen-activated protein kinase (p38MAPK) in the spinal microglia in a rat model of neuropathic pain. Soc Neurosci Abs 32:655.14
Tsuda M, Shigemoto-Mogami Y, Koizumi S, Mizokoshi A, Kohsaka S, Salter MW, Inoue K. 2003. $P2X_4$ receptors induced in spinal microglia gate tactile allodynia after nerve injury. Nature (in press).
Watkins LR, Milligan ED, Maier SF. 2001. Spinal cord glia: new players in pain. Pain 93:201–205.
Watkins LR, Martin D, Ulrich P, Tracey KJ, Maier SF. 1997. Evidence for the involvement of spinal cord glia in subcutaneous formalin induced hyperalgesia in the rat. Pain 71:225–235.
Winkelstein BA, Rutkowski MD, Sweitzer SM, Pahl JL, DeLeo JA. 2001. Nerve injury proximal or distal to the DRG induces similar spinal glial activation and selective cytokine expression but differential behavioral responses to pharmacologic treatment. J Comp Neurol 439:127–139.
Woolf CJ, Mannion RJ. 1999. Neuropathic pain: aetiology, symptoms, mechanisms, and management. Lancet 353:1959–1964.
Woolf CJ, Salter MW. 2000. Neuronal plasticity: increasing the gain in pain. Science 288:1765–1769.
Yaksh TL, Jessell TM, Gamse R, Mudge AW, Leeman SE. 1980. Intrathecal morphine inhibits substance P release from mammalian spinal cord in vivo. Nature 286:155–157.

J Pharmacol Sci 94, 112 – 114 (2004)

Journal of Pharmacological Sciences

Forum Minireview

ATP- and Adenosine-Mediated Signaling in the Central Nervous System: Chronic Pain and Microglia: Involvement of the ATP Receptor $P2X_4$

Kazuhide Inoue[1,2,*], Makoto Tsuda[1], and Schuichi Koizumi[3]

Divisions of [1]Biosignaling and [3]Pharmacology, National Institute of Health Sciences, 1-18-1 Kamiyoga, Setagaya-ku, Tokyo 158-8501, Japan
[2]Department of Molecular and System Pharmacology, Graduate School of Pharmaceutical Sciences, Kyushu University, 3-1-1 Maidashi, Higashi-ku, Fukuoka 812-8582, Japan

Received November 7, 2003; Accepted December 2, 2003

Abstract. We have been studying the role of ATP receptors in pain and already reported that activation of $P2X_{2/3}$ heteromeric channel/receptor in primary sensory neurons causes acutely tactile allodynia, one hallmark of neuropathic pain. We report here that tactile allodynia under the chronic pain state requires an activation of the $P2X_4$ ionotropic ATP receptor and p38 mitogen-activated protein kinase (MAPK) in spinal cord microglia. Two weeks after L5 spinal nerve injury, rats displayed a marked mechanical allodynia. In the rats, activated microglia were detected in the injured side of the dorsal horn and the level of the dually-phosphorylated active form of p38MAPK (phospho-p38MAPK) in these microglia was increased. Moreover, intraspinal administration of a p38MAPK inhibitor, SB203580, suppressed the allodynia. We also found that the expression level of $P2X_4$ was increased strikingly in spinal cord microgila after nerve injury and that pharmacological blockade or inhibition of the expression of $P2X_4$ reversed the allodynia. Taken together, our results demonstrate that activation of $P2X_4$ or p38MAPK in spinal cord microglia is necessary for tactile allodynia after nerve injury.

Keywords: ATP receptor, $P2X_4$, microglia, p38 mitogen-activated protein kinase, allodynia

Introduction

Injury of primary sensory neurons produces long-lasting abnormal hypersensitivity to normally innocuous stimuli, a phenomenon known as tactile allodynia (1, 2). Tactile allodynia is the most troublesome of the neuropathic pain syndromes in humans and the mechanisms by which nerve injury develops tactile allodynia have remained unknown (3).

The present article introduces our recent study (4, 5) revealing crucial roles of two molecules, expression and activation of which are highly restricted in microglia in the spinal cord, in neuropathic pain: p38 mitogen-activated protein kinase (p38MAPK) and $P2X_4$ receptor, a subtype of ionotropic ATP receptors.

*Corresponding author (affiliation #1). FAX: +81-3-3700-1349
E-mail: inoue@nihs.go.jp

p38MAPK was activated in spinal hyperactive microglia after nerve injury

Animals with spinal nerve injury displayed tactile allodynia. Paw withdrawal threshold (PWT) (ipsilateral side) to mechanical stimulation significantly decreased at 7 and 14 days. At day 7 and 14, the OX42 labelling was greater in the dorsal horn ipsilateral to the nerve injury. OX42-positive cells were more numerous and displayed hypertrophic morphology in the dorsal horn on the side of the nerve injury as compared with the contralateral side (4). To examine whether p38MAPK is activated in the spinal cord in rats that have developed tactile allodynia, we performed Western blot analysis using an antibody targeting the phosphorylated p38MAPK (phospho-p38MAPK). The band intensity of phospho-p38MAPK protein in the ipsilateral spinal cord dramatically increased 7 and 14 days after nerve injury compared with that in naive rat. Furthermore, we observed strong phospho-p38MAPK immunofluorescence

in the injury side of L5 dorsal spinal cord sections at 7 and 14 days after nerve injury (5). The bilateral difference in phospho-p38MAPK levels parallel with the emergence of the tactile allodynia. These results indicate that the p38MAPK is activated in the dorsal horn ipsilateral to the nerve injury, which may correlate with the nerve injury-induced tactile allodynia. We carried out double immunolabeling for phospho-p38MAPK and for cell type-specific markers to identify the type of cells and found that cells showing phospho-p38MAPK immunofluorescence was double labeled with OX42 but not with neuronal nuclei (NeuN) or glial fibrillary acidic protein (GFAP), indicating that activation of p38MAPK in the dorsal horn is highly restricted to microglia (5). OX42 recognizes the complement receptor type 3 (CR3), expression of which is greatly increased in hyperactive versus resting microglia after nerve injury (4 – 6). These results indicate that nerve injury induced a switch from the resting to the hyperactive phenotype in the population of microglia in the dorsal horn. We found that a marked phosphorylation of p38MAPK is observed in individual microglia in the ipsilateral dorsal horn (3.7-fold as compared with the contralateral side), particularly in hyperactive microglia that dramatically expressed OX42 (4). Therefore, we conclude that in the dorsal horn following nerve injury, hyperactive microglia are the cell type that activates p38MAPK and that the level of p38MAPK phosphorylation is dramatically increased in individual microglia.

p38MAPK activation in the spinal microglia caused development and maintenance of tactile allodynia

We examined whether intrathecal treatment with a potent inhibitor of p38MAPK, SB203580, alters the maintenance and development of tactile allodynia following nerve injury. Catheterized rats were treated with SB203580 (3 nmol/10 μL, n = 13) once at day 7 of the nerve injury. SB203580 treated-rats displayed a marked increase in PWT following nerve injury. When the rats were treated with SB203580 (30 nmol/10 μL, n = 9) once a day during 14 days from 0 day of the nerve injury, SB203580-treated rats showed only a slight decrease in PWT. These results suggest that inhibiting spinal p38MAPK activation in microglia by intrathecal treatment with inhibitor for p38MAPK suppresses the maintenance and development of tactile allodynia following spinal nerve injury.

The role of $P2X_4$ receptor in the tactile allodynia

We tested for the involvement of P2X receptors in the tactile allodynia by using ATP receptor blockers and found that tactile allodynia was reversed by the intrathecal administration of 2',3'-*O*-(2,4,6-trinitrophenyl) adenosine 5'-triphosphate (TNP-ATP) (30 nmol), an antagonist of P2X subtypes $P2X_{1-4}$, on day 7. Intrathecal administration of pyridoxial-phosphate-6-azophenyl-2',4'-disulphonic acid (PPADS), an antagonist of P2X subtypes $P2X_{1,2,3,5,7}$, but not of $P2X_4$, had no effect on either testing day. We observed no alteration in motor behaviour following TNP-ATP administration. These results together indicate that TNP-ATP caused a dose-dependent, reversible inhibition of allodynia on the nerve-injured side without a non-specific effect on motor or sensory functioning. At these intrathecal doses, PPADS is known to suppress nociceptive behaviors caused by intrathecal injection of the $P2X_{1,3}$ agonist α,β-methylene ATP. The lack of effect of PPADS on PWT together with the increase by TNP-ATP indicates that tactile allodynia caused by L5 nerve injury depends upon spinal P2X receptors that are sensitive to TNP-ATP and insensitive to PPADS. The pharmacological profile of these P2Xs is consistent with that of the $P2X_4$ subtype.

We found that $P2X_4$ protein in the ipsilateral spinal cord dramatically increased after L5 nerve injury. The increase in $P2X_4$ was detected as early as day 1 and the highest level was observed on day 14. The time-course of the change in $P2X_4$ level in the spinal cord and the bilateral difference in $P2X_4$ levels match the emergence of the tactile allodynia. We performed immunofluorescence on sections of the L5 spinal dorsal horn to examine the distribution of $P2X_4$. In the spinal cord ipsilateral to the nerve injury, we observed strong, punctate $P2X_4$ immunofluorescence in the dorsal horn on day 14. Furthermore, we found that cells showing $P2X_4$ immunofluorescence were not double-labelled for NeuN or GFAP. Almost all of the $P2X_4$-positive cells were double-labelled with OX42, indicating that $P2X_4$s were expressed in microglia.

Next we examined whether tactile allodynia following nerve injury is critically dependent upon functional $P2X_4$ in hyperactive microglia in the dorsal horn using an antisense oligodeoxynucleotide (ODN) targeting $P2X_4$. The nerve injury-induced allodynia was significantly suppressed in animals treated with $P2X_4$ antisense ODN as compared with that in animals treated with mismatch ODN (4). We also found that the level of $P2X_4$ protein in homogenates from the spinal cord of antisense ODN-treated rats was $32.0 \pm 4.8\%$ less than that of mismatch ODN-treated rats (4). These results indicate that intrathecal treatment with $P2X_4$ antisense ODN suppressed both the tactile allodynia and the increase in $P2X_4$ expression following nerve injury.

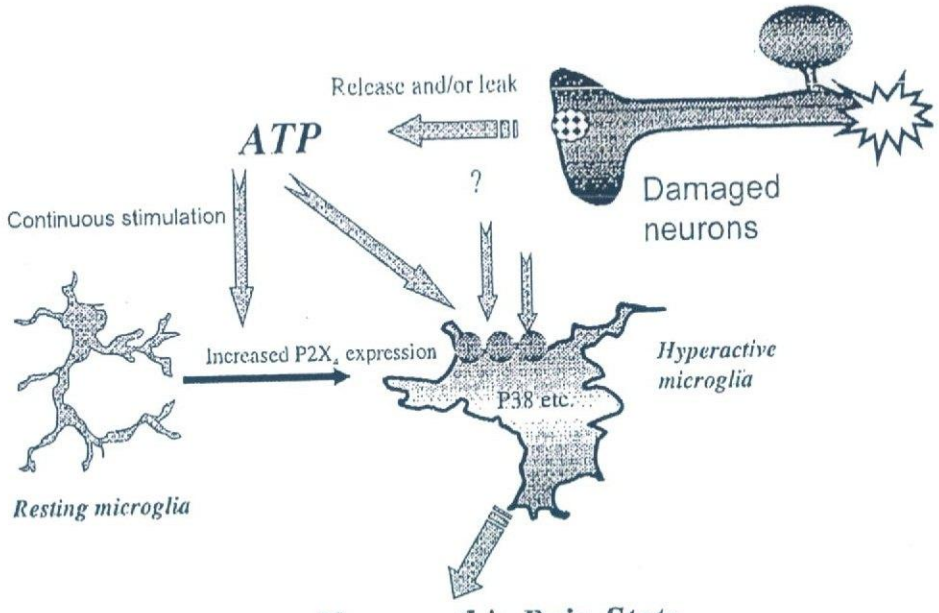

Fig. 1. Hypothesis: neuropathic pain after nerve injury. Tactile allodynia following nerve injury is critically dependent upon functional $P2X_4$ receptors in hyperactive microglia in the dorsal horn. ATP, which might be released or leaked from damaged neurons or astrocytes, stimulates resting microglia to be converted to hyperactive microglia. Hyperactive microglia increases the expression of $P2X_4$ receptors and p38-phosphorelation, resulting in tactile allodynia following nerve injury.

Conclusion

In the present article, we demonstrate that microglia in the spinal dorsal horn are converted to the hyperactive phenotype as a consequence of peripheral nerve injury and have dramatically expressed $P2X_4$ and activated p38MAPK. Also we suggested that the activation of p38MAPK and $P2X_4$ in spinal cord microglia are essential for allodynia after nerve injury (Fig. 1). The allodynia was reversed rapidly by pharmacological blockade of p38MAPK activation or inhibiting the expression of $P2X_4$ receptors, implying that nerve injury-induced pain hypersensitivity depends upon ongoing signaling via $P2X_4$ and/or p38MAPK, likely activated by ATP that may be released from primary sensory terminals (7 – 9), dorsal horn neurons (7, 10, 11), or dorsal horn astrocytes (12). Inhibition of $P2X_4$ expression, inhibiting the function of these receptors and/or p38MAPK in spinal microglia can be novel therapeutic approaches for treating tactile allodynia caused by nerve damage.

References

1 Woolf CJ, Mannion RJ. Neuropathic pain: aetiology, symptoms, mechanisms, and management. Lancet. 1999;353:1959–1964.
2 Scholz J, Woolf CJ. Can we conquer pain? Nat Neurosci. 2002;5:1062–1067.
3 Woolf CJ, Salter MW. Neuronal plasticity: increasing the gain in pain. Science. 2000;288:1765–1769.
4 Tsuda M, Shigemoto-Mogami Y, Koizumi S, et al. P2X4 receptors induced in spinal microglia gate tactile allodynia after nerve injury. Nature. 2003;424:778–783.
5 Tsuda M, Mizokoshi A, Shigemoto-Mogami Y, Koizumi S, Inoue K. Activation of p38 mitogen-activated protein kinase in spinal hyperactive microglia contributes to pain hypersensitivity following peripheral nerve injury. Glia. 2004;45:89–95.
6 Aldskogius H, Kozlova EN. Central neuron-glial and glial-glial interactions following axon injury. Prog Neurobiol. 1998;55:1–26.
7 Sawynok J, Downie JW, Reid AR, Cahill CM, White TD. ATP release from dorsal spinal cord synaptosomes: characterization and neuronal origin. Brain Res. 1993;610:32–38.
8 Li P, Calejesan AA, Zhuo M. ATP P2X receptors and sensory synaptic transmission between primary afferent fibers and spinal dorsal horn neurons in rats. J Neurophysiol. 1998;80:3356–3360.
9 Nakatsuka T, Gu JG. ATP P2X receptor-mediated enhancement of glutamate release and evoked EPSCs in dorsal horn neurons of the rat spinal cord. J Neurosci. 2001;21:6522–6531.
10 Bardoni R, Goldstein PA, Lee CJ, Gu JG, MacDermott AB. ATP P2X receptors mediate fast synaptic transmission in the dorsal horn of the rat spinal cord. J Neurosci. 1997;17:5297–5304.
11 Jo YH, Schlichter R. Synaptic corelease of ATP and GABA in cultured spinal neurons. Nat Neurosci. 1999;2:241–245.
12 Fam SR, Gallagher CJ, Salter MW. $P2Y_1$ purinoceptor-mediated Ca^{2+} signaling and Ca^{2+} wave propagation in dorsal spinal cord astrocytes. J Neurosci. 2000;20:2800–2808.

Biochem. J. (2004) 380, 329–338 (Printed in Great Britain)

Ca^{2+} waves in keratinocytes are transmitted to sensory neurons: the involvement of extracellular ATP and $P2Y_2$ receptor activation

Schuichi KOIZUMI*, Kayoko FUJISHITA†, Kaori INOUE‡, Yukari SHIGEMOTO-MOGAMI†, Makoto TSUDA† and Kazuhide INOUE†§[1]

*Division of Pharmacology, National Institute of Health Sciences, 1-18-1 Kamiyoga, Setagaya, Tokyo 158-8501, Japan, †Division of Biosignaling, National Institute of Health Sciences, 1-18-1 Kamiyoga, Setagaya, Tokyo 158-8501, Japan, ‡Shiseido Research Center, 2-12-1 Fukuura, Kanazawa-ku, Yokohama 236-8643, Japan, and §Graduate School of Pharmaceutical Sciences, Kyushu University, 3-1-1 Maidashi, Fukuoka 812-8582, Japan

ATP acts as an intercellular messenger in a variety of cells. In the present study, we have characterized the propagation of Ca^{2+} waves mediated by extracellular ATP in cultured NHEKs (normal human epidermal keratinocytes) that were co-cultured with mouse DRG (dorsal root ganglion) neurons. Pharmacological characterization showed that NHEKs express functional metabotropic $P2Y_2$ receptors. When a cell was gently stimulated with a glass pipette, an increase in $[Ca^{2+}]_i$ (intracellular Ca^{2+} concentration) was observed, followed by the induction of propagating Ca^{2+} waves in neighbouring cells in an extracellular ATP-dependent manner. Using an ATP-imaging technique, the release and diffusion of ATP in NHEKs were confirmed. DRG neurons are known to terminate in the basal layer of keratinocytes. In a co-culture of NHEKs and DRG neurons, mechanical-stimulation-evoked Ca^{2+} waves in NHEKs caused an increase in $[Ca^{2+}]_i$ in the adjacent DRG neurons, which was also dependent on extracellular ATP and the activation of $P2Y_2$ receptors. Taken together, extracellular ATP is a dominant messenger that forms intercellular Ca^{2+} waves in NHEKs. In addition, Ca^{2+} waves in NHEKs could cause an increase in $[Ca^{2+}]_i$ in DRG neurons, suggesting a dynamic cross-talk between skin and sensory neurons mediated by extracellular ATP.

Key words: ATP, Ca^{2+} wave, cross-talk, dorsal root ganglion neuron, keratinocyte, $P2Y_2$ receptor.

INTRODUCTION

The skin is the largest organ of the body and is exposed to multiple external stimuli. It protects water-rich internal organs from harmful environmental factors such as dryness, chemicals, noxious heat and UV irradiation. In addition, the skin is exposed to various substances such as ATP, bradykinin and histamine after skin injury and during inflammatory skin diseases and allergic reactions respectively. Thus the skin expresses various sensors for environmental stimuli [1,2] or neurotransmitters [3–6]. Various environmental stimuli or neurotransmitters often cause changes in $[Ca^{2+}]_i$ (intracellular Ca^{2+} concentration) in the skin [5,7,8]. Ca^{2+} dynamics play an important role in the homoeostasis of the skin epidermis, the outermost part of skin tissue; the skin epidermis tunes the balance between the proliferation and differentiation of epidermal keratinocytes [1,9].

Propagation of intercellular Ca^{2+} waves from one cell to another is a well-known phenomenon in non-excitable cells such as astrocytes [10,11], hepatocytes [12], epithelial cells [13] and endothelial cells [14]. These cells lack regenerative electrical action potentials but use Ca^{2+} waves for their long-range communications. In astrocytes, extracellular molecules such as glutamate [11] and ATP [15], rather than gap junction via connexin43, have been suggested to be important factors for the Ca^{2+} wave [16]. Epidermal keratinocytes are non-excitable cells and do not produce action potentials. However, the mechanisms of intercellular Ca^{2+} waves in keratinocytes have received only limited attention. Given that Ca^{2+} waves in keratinocytes are mediated by the release of extracellular molecules, such signals may also affect the activity of surrounding cells such as sensory neurons. Although junctions have not been found between keratinocytes and sensory termini, ultrastructural studies have shown that keratinocytes contact DRG (dorsal root ganglion) nerve fibres through membrane–membrane apposition [17,18]. Immunostaining of the neuronal marker PGP 9.5 (protein gene product 9.5) revealed the presence of free nerve endings at epidermal keratinocytes [19]. There is indirect evidence that keratinocytes communicate with sensory neurons via extracellular molecules. For example, although dissociated DRG neurons can be directly activated by heat and cold, warm responses have only been demonstrated in experiments where skin–nerve connectivity is intact [20,21]. A warmth sensor, TRPV3, is present in epidermal keratinocytes, but not in sensory neurons [19]. Sensory neurons themselves sense various external stimuli, but there might be skin-derived regulatory mechanisms by which sensory signalling is modulated.

In the present study, we report that mechanical stimulation of NHEKs (normal human epidermal keratinocytes) with a glass pipette induces propagating Ca^{2+} waves in an extracellular ATP-dependent manner. NHEKs release ATP and, in turn, the released ATP activates $P2Y_2$ receptors in NHEKs. We also demonstrate that, in a co-culture of NHEKs and DRG neurons, such extracellular ATP-dependent Ca^{2+} waves in NHEKs cause increases in $[Ca^{2+}]_i$ even in the adjacent DRG neurons, suggesting that dynamic cross-talk occurs between keratinocytes and DRG neurons via extracellular ATP.

EXPERIMENTAL

Cell culture

NHEKs were obtained as cryopreserved first passage cells from neonatal foreskins (Kurabo, Osaka, Japan). Cells were plated on collagen-coated coverslips and then cultured in serum-free

Abbreviations used: ATPγS, adenosine 5′-[γ-thio]triphosphate; BSS, balanced salt solution; $[Ca^{2+}]_i$, intracellular Ca^{2+} concentration; DRG, dorsal root ganglion; αβmeATP, α,β-methylene-ATP; 2meSADP, 2methyl-thio-ADP; NHEK, normal human epidermal keratinocyte; RT, reverse transcriptase.

[1] To whom correspondence should be addressed (e-mail inoue@nihs.go.jp).

keratinocyte growth medium consisting of Humedia-KB2 (Kurabo), supplemented with bovine pituitary extract (0.4 %, v/v), human recombinant epidermal growth factor (0.1 ng/ml), insulin (10 μg/ml), cortisol (0.5 μg/ml), gentamicin (50 μg/ml) and amphotericin B (50 ng/ml). The media were replaced every 2–3 days. For co-culturing NHEKs and mouse DRG neurons, NHEKs were seeded on mitomycin C (4 μg/ml)-treated 3T3-J2 fibroblast feeder layers (2×10^5 cells/cm^2) in 'Green' medium [3:4 Dulbecco's minimal Eagle's medium and 1:4 Ham's F12, supplemented with 10 % (v/v) foetal bovine serum, 20 mM Hepes, 100 units/ml penicillin, 100 μg/ml streptomycin, 5 μg/ml insulin, 0.5 μg/ml cortisol, 0.1 nM cholera enterotoxin, 0.01 μg/ml recombinant human epidermal growth factor, 0.25 μg/ml amphotericin B and 180 μM adenine]. The dissociated mouse DRG neurons were seeded, 2 days after the seeding of NHEKs, on the cell layer and then cultured for an additional 1 week.

Ca^{2+} imaging in single NHEKs

Changes in $[Ca^{2+}]_i$ in single cells were measured by the fura 2 method as described by Grynkiewicz et al. [22] after minor modifications [23]. In brief, the culture medium was replaced with BSS (balanced salt solution) of the following composition (mM): NaCl 150, KCl 5.0, $CaCl_2$ 1.8, $MgCl_2$ 1.2, Hepes 25 and D-glucose 10 (pH 7.4). Cells were loaded with fura 2 by incubation with 5 μM fura 2/AM (fura 2 acetoxymethyl ester; Molecular Probes, Eugene, OR, U.S.A.) at room temperature (20–22 °C) in BSS for 45 min, followed by washing with BSS and a further 15 min incubation to allow de-esterification of the loaded dye. The coverslips were mounted on an inverted epifluorescence microscope (TMD-300; Nikon, Tokyo, Japan) equipped with a 75 W xenon lamp and band-pass filters of 340 and 360 nm wavelengths. Measurements were carried out at room temperature. Images were recorded by a high-sensitivity silicon intensifier target camera (C-2741-08; Hamamatsu Photonics, Hamamatsu, Japan) and the image data were regulated by a Ca^{2+} analysing system (Furusawa Laboratory Appliance, Kawagoe, Japan). The absolute $[Ca^{2+}]_i$ was estimated from the ratio of emitted fluorescences (F_{340}/F_{360}) according to a calibration curve obtained by using Ca^{2+} buffers. For Ca^{2+}-free experiments, Ca^{2+} was removed from the BSS (0 Ca^{2+}). Drugs were dissolved in BSS and applied by superfusion. For mechanical stimulation, a single NHEK in the centre of the microscopic field was probed with a glass micropipette using a micromanipulator (Narishige, Tokyo, Japan). Under visible light, the tip of the micropipette was positioned approx. 2 μm over the cell to be stimulated. When sampling, the micropipette was rapidly lowered by approx. 2 μm and then rapidly returned to its original position. If the stimulated cell showed no increase in fluorescence, the pipette was lowered again until stimulation was seen. If the stimulated cell showed any sign of damage (dye leakage or abnormal morphology), the experiment was eliminated. For confocal Ca^{2+} imaging, the cells were loaded with 5 μM fura 4/AM for 30–40 min at room temperature and then mounted on a microscope (TE-2000; Nikon) equipped with a CSU-10 laser-scanning unit (Yokogawa, Tokyo, Japan) and a high-sensitivity CCD (charge-coupled-device) camera (ORCA-ER; Hamamatsu Photonics), as described previously [24]. To compensate for the uneven distribution of the fluo-4, self-ratios were calculated ($R_s = F/F_0$), which were subsequently converted into Ca^{2+} concentration using the following equation:

$$[Ca^{2+}]_i = R_s K_d / [(K_d / [Ca^{2+}]_{rest}) - R_s]$$

The K_d value of fluo-4 for NHEKs was taken to be 706 nM as determined by an *in vivo* calibration method.

Table 1 Primer pairs and end-products

Amplicon shows the base pairs of the PCR end-product.

Gene	Primer	Size (-mer)	Amplicon (bp)
P2Y1	F: 5′-GAGGGCCCGGCTTGATT-3′	17	67
	R: 5′-ATACGTGGCATAAACCCTGTCA-3′	22	
P2Y2	F: 5′-TGGTGCGCTTCCTCTTCTACA-3′	21	72
	R: 5′-ACCGGTGCACGCTGATG-3′	17	
P2Y4	F: 5′-TCATGGCTCGTCGCCTGTA-3′	19	67
	R: 5′-AGAGAGCGGAGGCGAGAAG-3′	19	
P2Y6	F: 5′-CCTGCCCACAGCCATCTT-3′	18	116
	R: 5′-CAGTGAGAGCCATGCCATAGG-3′	21	
P2Y11	F: 5′-CTGCCCTGCCAACTTCTTG-3′	19	78
	R: 5′-ACCAGTATGGGCCACAGGAA-3′	20	
P2Y12	F: 5′-CCTTTCCATTTTGCCCGAAT-3′	20	74
	R: 5′-GTATTTTCAGCAGTGCAGTCAAAGA-3′	25	

Imaging of ATP release

ATP release from NHEKs was detected with a luciferin–luciferase bioluminescence assay. After an initial 30 min superfusion period, superfusion was stopped and the cell chamber was filled with BSS containing a luciferase reagent (ATP bioluminescence assay kit CLS II; Roche Diagnostics, Mannheim, Germany). ATP bioluminescence was detected and visualized with a VIM camera (C2400-35; Hamamatsu Photonics) using an integration time of 30 s. The absolute ATP concentration was estimated using a standard ATP solution (ATP bioluminescence assay kit CLS II).

Immunocytochemistry

Cultures were fixed with 4 % (w/v) paraformaldehyde for 10 min and soaked in PBS solution. Cells were incubated with primary antibodies (rabbit anti-peripherin antibody, 1:200; Chemicon, Temecula, CA, U.S.A.; monoclonal mouse anti-cytokeratin14 antibody, 1:100; Cymbus Biotechnology, Chandlers Ford, U.K.), dissolved in blockace solution (1:10 dilution; Dainippon, Osaka, Japan) for 1 h at room temperature and then covered with diluted (1:500) secondary fluorescent antiserum solution (Alexa488- and Alexa546-conjugated rabbit and mouse anti-IgGs respectively) and kept at 4 °C overnight. Then, the cells were washed three times with PBS containing 0.05 % Tween 20 for 15 min and mounted with Vectashied (Vector Laboratories, Burlingame, CA, U.S.A.). Images were obtained by confocal microscopy (Radiance 2000; Bio-Rad Japan, Tokyo, Japan).

Reverse transcriptase (RT)–PCR of P2 receptors

The total RNA was isolated and purified using RNeasy mini kits (Qiagen) according to the manufacturer's instructions. RT–PCR amplifications were performed using Taqman One-step RT–PCR Master Mix Reagents and 200 nM of each P2 receptor-specific primer. Using the software Primer Express (Applied Biosystems, Tokyo, Japan), clone-specific primers were designed to recognize human P2Y receptors, as shown in Table 1. All primers had similar melting temperatures for running the same cycling programme for all samples. RT–PCR was performed by 30 min reverse transcription at 48 °C, 10 min AmpliTaq Gold activation at 95 °C, then 15 s denaturation at 95 °C and, finally, 1 min annealing and elongation at 60 °C for 40 cycles in a PRISM 7700 (Applied Biosystems). To exclude contamination by unspecific PCR products such as primer dimers, melting curve analysis was performed on all the final PCR products after the cycling procedure.

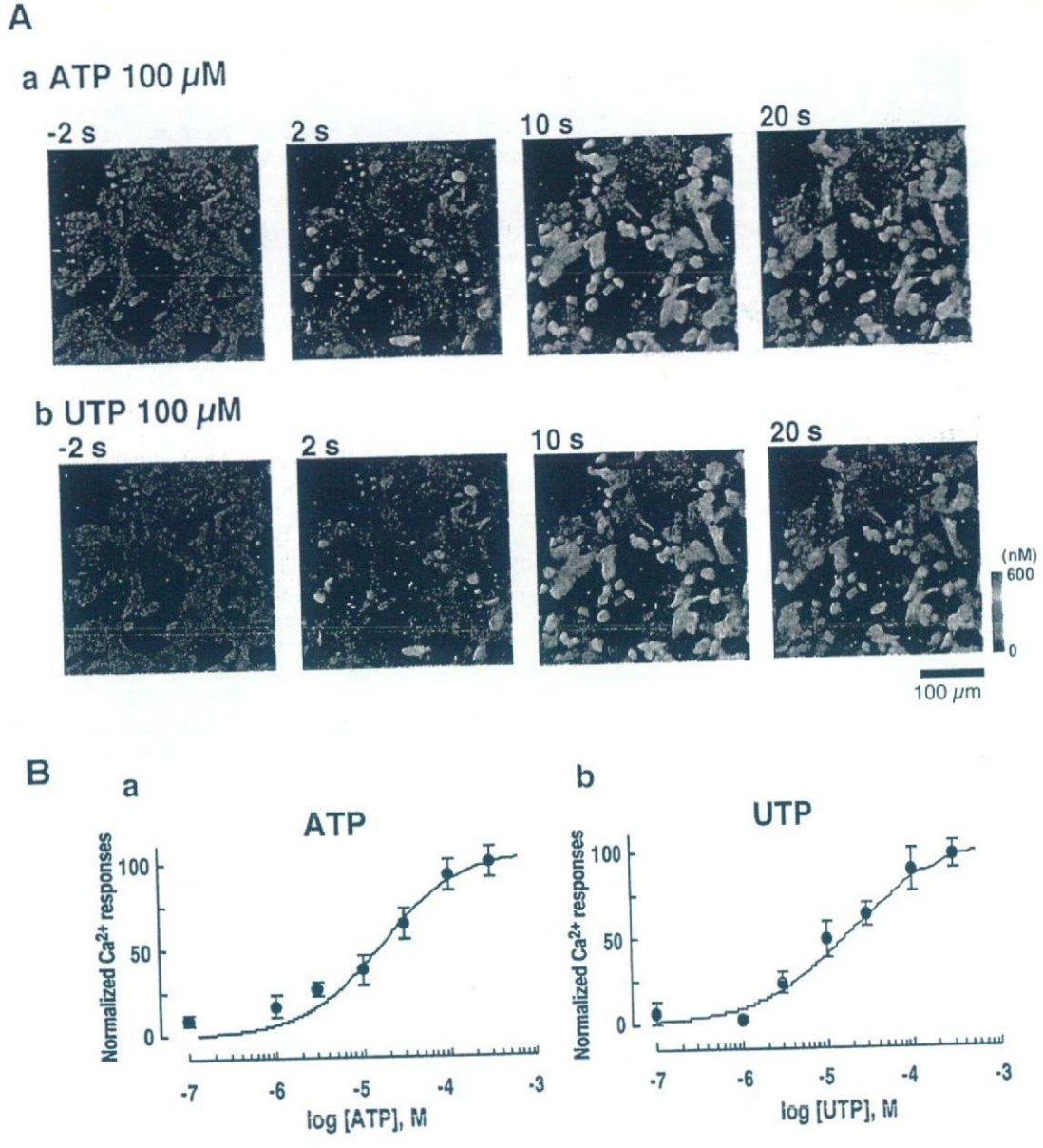

Figure 1 Increases in $[Ca^{2+}]_i$ evoked by both applied ATP and UTP in NHEKs

(**A**) Sequential pseudo colour images of Ca^{2+} responses to 100 μM ATP (**a**) and UTP (**b**). Images were obtained from a confocal laser microscope, showing self-ratios of fluo-4 fluorescence. Images were recorded 2 s before (− 2 s) and 2, 10 and 20 s after ATP or UTP application. (**B**) Concentration–response curves for (**a**) ATP- and (**b**) UTP-evoked increases in $[Ca^{2+}]_i$ in NHEKs. Increases in $[Ca^{2+}]_i$ in NHEKs were monitored by ratiometric fura 2 fluorescence ($\Delta F_{340}/F_{360}$) and were then converted into absolute value of $[Ca^{2+}]_i$ using a standard calibration curve. The maximum $[Ca^{2+}]_i$ increase was observed when cells were stimulated with 300 μM ATP (**a**) or UTP (**b**). The increase in $[Ca^{2+}]_i$ at each ATP or UTP concentration was normalized by the maximum increase in $[Ca^{2+}]_i$. Results are the means ± S.E.M. for 28–73 cells tested. Both the ATP- and UTP-evoked concentration–response curves were almost identical with the ED_{50} values of 21 and 20 μM respectively.

Statistics

Experimental results are expressed as means ± S.E.M. and statistical differences between two groups were determined by Student's *t* test.

RESULTS

Characterization of ATP-evoked $[Ca^{2+}]_i$ increases in NHEKs

Exogenously applied ATP induced an increase in $[Ca^{2+}]_i$ in NHEKs with an ED_{50} value of 21 μM (Figures 1Aa and 1Ba). UTP also caused an increase in $[Ca^{2+}]_i$ in the cells, with a similar ED_{50} value of 20 μM (Figures 1Ab and 1Bb). The ATP-evoked increase in $[Ca^{2+}]_i$ was almost independent of the extracellular Ca^{2+}, but was decreased by U73122, an inhibitor of phospholipase C, and thapsigargin, an inhibitor of Ca^{2+}-ATPase of Ca^{2+} stores, suggesting the involvement of inositol 1,4,5-trisphosphate/phospholipase C-linked metabotropic P2Y receptors in the Ca^{2+} responses (Figure 2A). UTP activates UTP-preferring $P2Y_2$ and $P2Y_4$ receptors, and UDP, generated by de-phosphorylation of UTP, stimulates $P2Y_6$ receptors. We therefore analysed the expression of mRNAs for these P2Y receptors using an RT–PCR method and detected the signals for $P2Y_1$, $P2Y_2$ and $P2Y_{11}$ receptors (Figure 2B, inset). Each PCR product possessed the predicted length (Table 1). Signals for $P2Y_4$, $P2Y_6$ and $P2Y_{12}$ were hardly detected in NHEKs. To confirm the functional responses

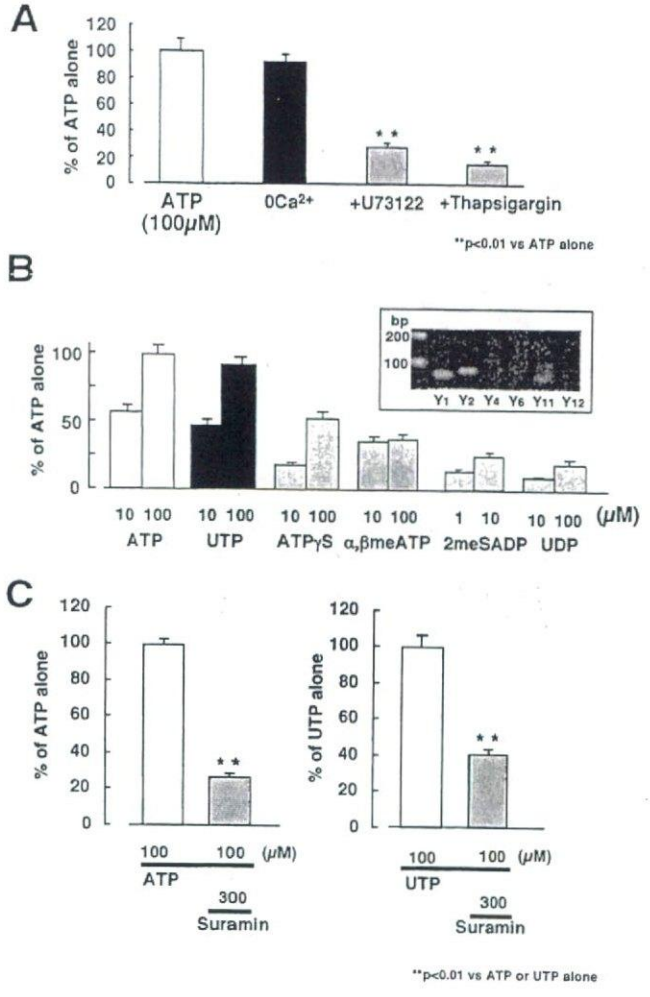

Figure 2 Characterization of P2 receptor-mediated Ca^{2+} responses in NHEKs

The ATP-evoked increases in $[Ca^{2+}]_i$ in NHEKs were characterized. Increases in $[Ca^{2+}]_i$ in cells were calculated by ratiometric fura 2 fluorescence ($\Delta F_{340}/F_{360}$) and a standard calibration curve. Values were normalized by the Ca^{2+} response at 100 μM ATP or UTP and were expressed as a percentage of ATP or UTP alone (**C**, right). (**A**) ATP was applied to NHEKs for 20 s and the U73122 (5 μM) was applied to the cells 10 min before and during the ATP application. Thapsigargin (100 nM) was applied to the cells 5 min before and during the ATP application. Results were obtained from 28 to 61 cells tested (at least two independent experiments). $^{**}P < 0.01$, significant differences from the response evoked by ATP alone. (**B**) Pharmacological characterization of Ca^{2+} responses in NHEKs. UTP was as potent as ATP. ATPγS and $\alpha\beta$meATP were much less potent than ATP. 2meSADP and UDP caused only slight increases in $[Ca^{2+}]_i$ in NHEKs. Results were obtained from 24 to 57 cells tested (at least two independent experiments). The inset shows the agarose-gel electrophoresis, indicating expression of mRNAs for various P2Y receptors in NHEKs. (**C**) Suramin (300 μM) inhibited both the ATP- and UTP-evoked increases in $[Ca^{2+}]_i$ in NHEKs. Results were obtained from 117 to 128 cells tested (four independent experiments). $^{**}P < 0.01$, significant differences from the response evoked by ATP or UTP alone.

of these P2Y receptors, we further performed pharmacological analysis using the fura 2-based Ca^{2+} imaging methods. The increase in $[Ca^{2+}]_i$ evoked by UTP was almost identical with that evoked by ATP. Both the $P2Y_{11}$ receptor agonist ATPγS (adenosine 5′-[γ-thio]triphosphate) and the P2X receptor agonist $\alpha\beta$meATP (α,β-methylene-ATP) caused increases in $[Ca^{2+}]_i$, but they were less than those caused by ATP or UTP. 2meSADP (2methyl-thio-ADP), a $P2Y_1$ receptor agonist, and UDP, a $P2Y_6$ receptor agonist, evoked only slight increases in $[Ca^{2+}]_i$ in the cells. The potency rank order for the Ca^{2+} response was ATP = UTP > ATPγS > $\alpha\beta$meATP > 2meSADP > UDP (Figure 2B). Cross-desensitization was observed between ATP and UTP (results not shown). Suramin at 300 μM decreased both the ATP- and UTP-evoked $[Ca^{2+}]_i$ increases (Figure 2C: 29.8 $\pm$ 2.2 % of ATP alone, $n = 128$; 44.1 $\pm$ 2.7 % of UTP alone, $n = 117$). These results suggest that the $P2Y_2$ receptors were responsible for these responses.

Propagating Ca^{2+} waves in response to mechanical stimulation in NHEKs

When an NHEK was stimulated with a glass pipette, an increase in $[Ca^{2+}]_i$ in the cell was observed, followed by induction of a propagating Ca^{2+} wave after a time lag in neighbouring NHEKs (Figure 3A, upper panels). The findings that the same cell evoked a Ca^{2+} response to repeated (up to three times) mechanical stimulations (results not shown) and that the cell showed some sign of damage suggest that mechanical stimulation would not cause injury to the stimulated cells. The propagation of Ca^{2+} waves was abolished by 80 units/ml apyrase [grade III; Figures 3A (lower panels) and 3B]. Both the P2 receptor antagonists suramin (300 μM) and pyridoxal phosphate-6-azophenyl-2′,4′-disulphonic acid (100 μM) significantly inhibited the Ca^{2+} wave; however, adenosine 3′-phosphate 5′-phosphosulphate (100 μM), an antagonist to the $P2Y_1$ receptor, and 1-octanol (500 μM), an inhibitor of gap junction, did not affect the Ca^{2+} waves (Figure 3C). The $[Ca^{2+}]_i$ increase in the stimulated cells was not affected by these antagonists. All these findings suggest that the propagating Ca^{2+} wave in response to mechanical stimulation in NHEKs was mediated by extracellular ATP and mainly by the activation of $P2Y_2$ receptors.

Release and diffusion of ATP from NHEKs

To demonstrate directly the stimulus-evoked release of ATP from NHEKs, we modified the luciferin–luciferase chemiluminescence bioassay for detecting ATP levels by using a high-sensitivity single photon-counting camera to correlate photon counts with increases in extracellular ATP. NHEKs were bathed in a solution containing the luciferin–luciferase reagents and photons were counted before and 30 s after mechanical stimulation of an NHEK. Figure 4(a) shows a phase-contrast image of a microscopic field, and Figures 4(b) and 4(c) show bioluminescence images before and after mechanical stimulation in the same field respectively. The standard calibration curve obtained under this condition showed a high correlation between the bioluminescence intensity and the ATP concentration with a correlation coefficient of 0.986 over a concentration range of 10 nM–10 μM (Figure 4d). The resting level of the bioluminescence signal was very low; then, it was increased to a level sufficient to evoke increases in $[Ca^{2+}]_i$ in NHEKs (3.2 $\pm$ 0.91 μM, $n = 12$) in response to mechanical stimulation for 30 s (Figures 4c and 4f). To visualize the spatiotemporal dynamics of the stimulus-evoked release of ATP from NHEKs, the extracellular ATP levels were plotted as pseudo colour images using the Excel 2-D surface plot program. As shown in Figures 4(e) and 4(f), the levels of extracellular ATP after mechanical stimulation were highest at the site of stimulation and decreased concentrically. These results show that the mechanically evoked Ca^{2+} waves were well associated with the release of ATP from NHEKs and the activation of $P2Y_2$ receptors.

Ca^{2+} waves in NHEKs activate increase in $[Ca^{2+}]_i$ in DRG neurons

As described in the Introduction section, sensory neurons terminate in the skin. Hence, a co-culture of NHEKs and mouse

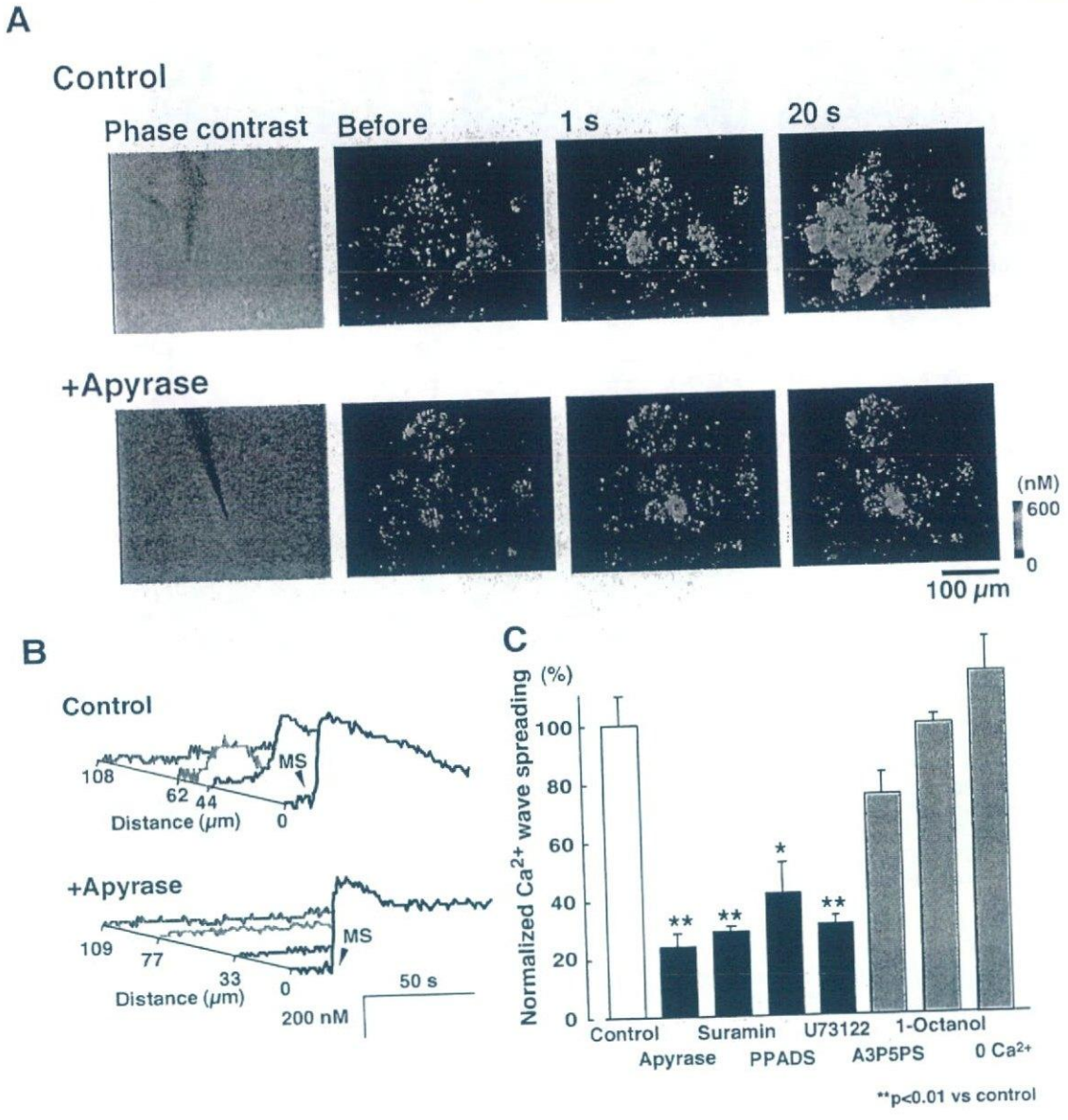

Figure 3 Propagation of Ca^{2+} waves in response to mechanical stimulation in NHEKs

(**A**) Phase-contrast (left) and pseudo $[Ca^{2+}]_i$ images of a field of cultured NHEKs in the absence (upper panels) and presence (lower panels) of apyrase (80 units/ml). Increase in $[Ca^{2+}]_i$ was estimated by ratiometric fura 2 fluorescence ($\Delta F_{340}/F_{360}$) and was then converted into absolute $[Ca^{2+}]_i$ using a standard calibration curve. A single NHEK was mechanically stimulated. (**B**) Plots of $[Ca^{2+}]_i$ as a function of time in four individual NHEKs in the microscopic field. The plots for the non-stimulated cells (blue, green and red traces) horizontally regressed in proportion to their distance from the stimulated cell (black traces) as indicated by the scale bar. In a control experiment, mechanical stimulation of NHEK 1 (black trace) resulted in the induction of a Ca^{2+} wave in adjacent cells after a time lag (upper traces). However, in the presence of apyrase (80 units/ml), mechanical stimulation failed to cause increases in $[Ca^{2+}]_i$ in the surrounding NHEKs (lower traces). The diameter of the spreading distance of the Ca^{2+} wave was calculated in the absence and presence of various chemicals and is summarized in (**C**). The average diameter of the Ca^{2+} wave under the control condition was 93.4 ± 9.7 μm ($n = 12$). Suramin (300 μM), pyridoxal phosphate-6-azophenyl-2′,4′-disulphonic acid (PPADS; 100 μM) and U73122 (5 μM) also abolished the propagation of Ca^{2+} waves, but adenosine 3′-phosphate 5′-phosphosulphate (A3P5PS; 100 μM), 1-octanol (500 μM) or removal of extracellular Ca^{2+} (0 Ca^{2+}) failed to inhibit the mechanical-stimulation-evoked Ca^{2+} wave in NHEKs ($n = 8$–12).

DRG neurons was prepared as described in the Experimental section. Figure 5(A) shows an immunohistochemical image of anti-cytokeratin14 (red) and anti-peripherin (green) antibodies, which are markers for the basal layer of keratinocytes and small-sized DRG neurons respectively. When stimulated with 80 mM KCl, almost all peripherin-positive DRG neurons (Figure 5B, green traces) exhibited increases in $[Ca^{2+}]_i$, whereas cytokeratin14-positive NHEKs (Figure 5B, red trace) did not. Both ATP (100 μM) and UTP (100 μM) caused increases in $[Ca^{2+}]_i$ in 71 % of the small-sized DRG neurons (37 out of 52 cells tested; $dF/F_0 = 6.3 \pm 0.8$ for ATP and 5.8 ± 0.6 for UTP; $n = 37$ in four separate experiments), and 73 % of NHEKs (58 out of 79 cells tested; $dF/F_0 = 5.1 \pm 0.7$ for ATP and 4.3 ± 0.4 for UTP; $n = 58$ in four separate experiments). The UTP-evoked increases in $[Ca^{2+}]_i$ in both types of cells were reproducible, and the first and second UTP-evoked responses were almost identical. The average diameter of the small-sized DRG neurons was 21.8 ± 3.5 μm. Suramin (100 μM) inhibited the UTP-evoked increases in $[Ca^{2+}]_i$ in both types of cells (DRG neurons, 10.2 ± 2.1 % of UTP alone, $n = 37$; NHEKs, 32.1 ± 4.6 % of UTP alone, $n = 58$). Thus

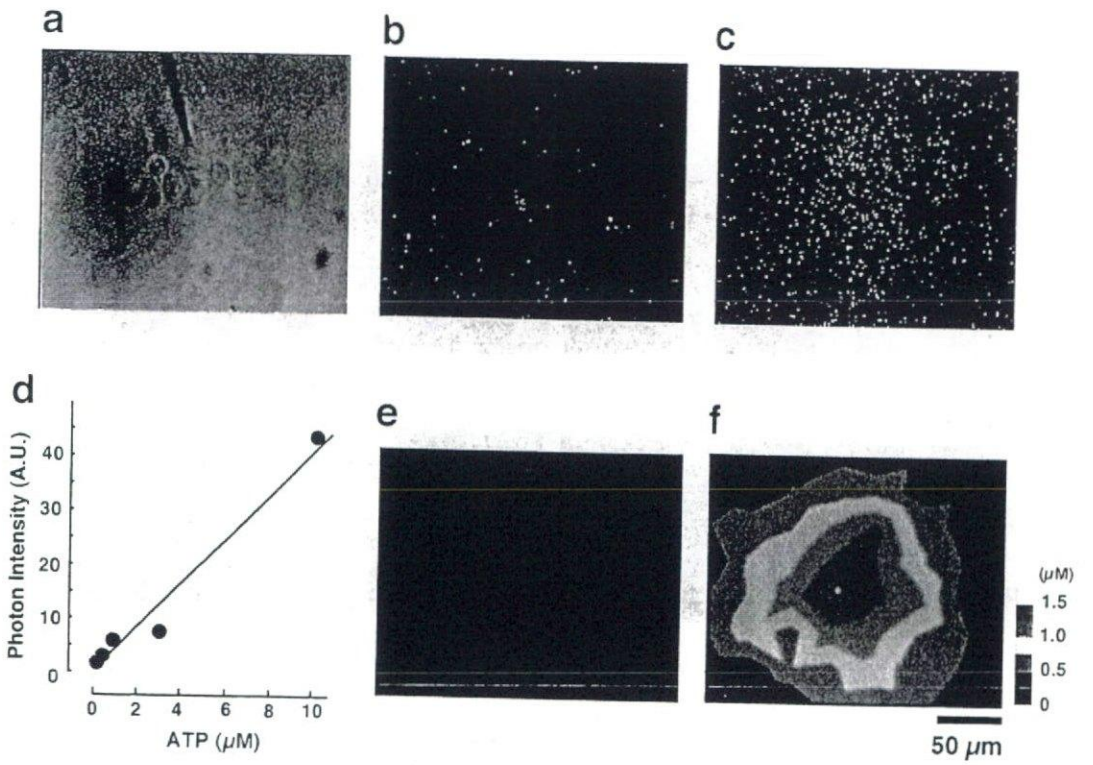

Figure 4 Visualization of release of ATP from NHEKs

The images show photon counts (yellow dots) in a field of NHEKs bathed in luciferin–luciferase reagent before (**b**) and after (**c**) mechanical stimulation. The position of pipette is shown in a phase-contrast image of NHEKs (**a**). (**d**) A typical bioluminescence intensity–ATP concentration relationship under these conditions. Various concentrations of ATP standard solution were injected in the presence of the luciferin–luciferase reagent, and photons were then accumulated for 30 s. (**e**, **f**) Spatial distribution of photon counts of mechanical stimulation shown as a two-dimensional pseudo colour surface plot. Scale bar, 50 μm for images **a**–**c**.

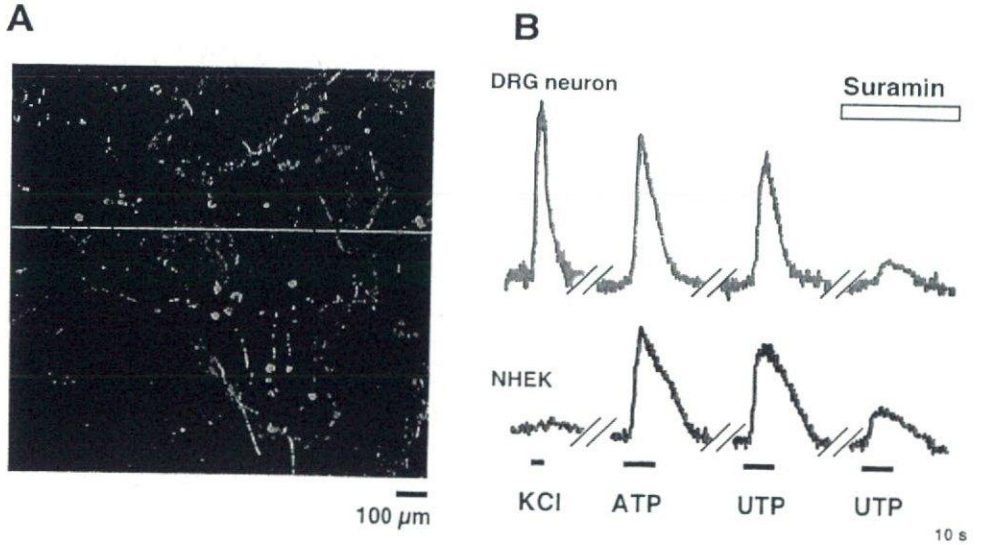

Figure 5 Immunohistochemical staining of DRG neurons and NHEKs

(**A**) After some Ca^{2+} imaging experiments, cells were fixed and stained with anti-cytokeratin14 and anti-peripherin antibodies for confirming NHEKs and small-sized DRG neurons respectively. (**B**) Representative Ca^{2+} responses obtained from sell-ratios of fluo-4 fluorescence in anti-peripherin-positive DRG neuron (green) and anti-cytokeratin14-positive NHEK (red). First, cells were stimulated with 80 mM KCl for 3 s. Then, they were stimulated with 100 μM ATP for 10 s and 100 μM UTP for 10 s separated by 5 min. Finally, UTP (100 μM) was applied to the cells in the presence of 100 μM suramin. Both ATP and UTP caused increases in $[Ca^{2+}]_i$ in approx. 71 % of the DRG neurons (37 out of 52 cells tested) and in 73 % of the NHEKs (58 out of 79 cells tested) in the co-cultured cells.

most of the small-sized neurons also expressed UTP-preferring suramin-sensitive P2Y receptors, presumably $P2Y_2$ receptors. In the co-culture of NHEKs and DRG neurons, mechanical stimulation of a single NHEK produced a propagating Ca^{2+} wave in adjacent NHEKs in an extracellular ATP-dependent manner (Figure 6A). Interestingly, this Ca^{2+} wave in the NHEKs was

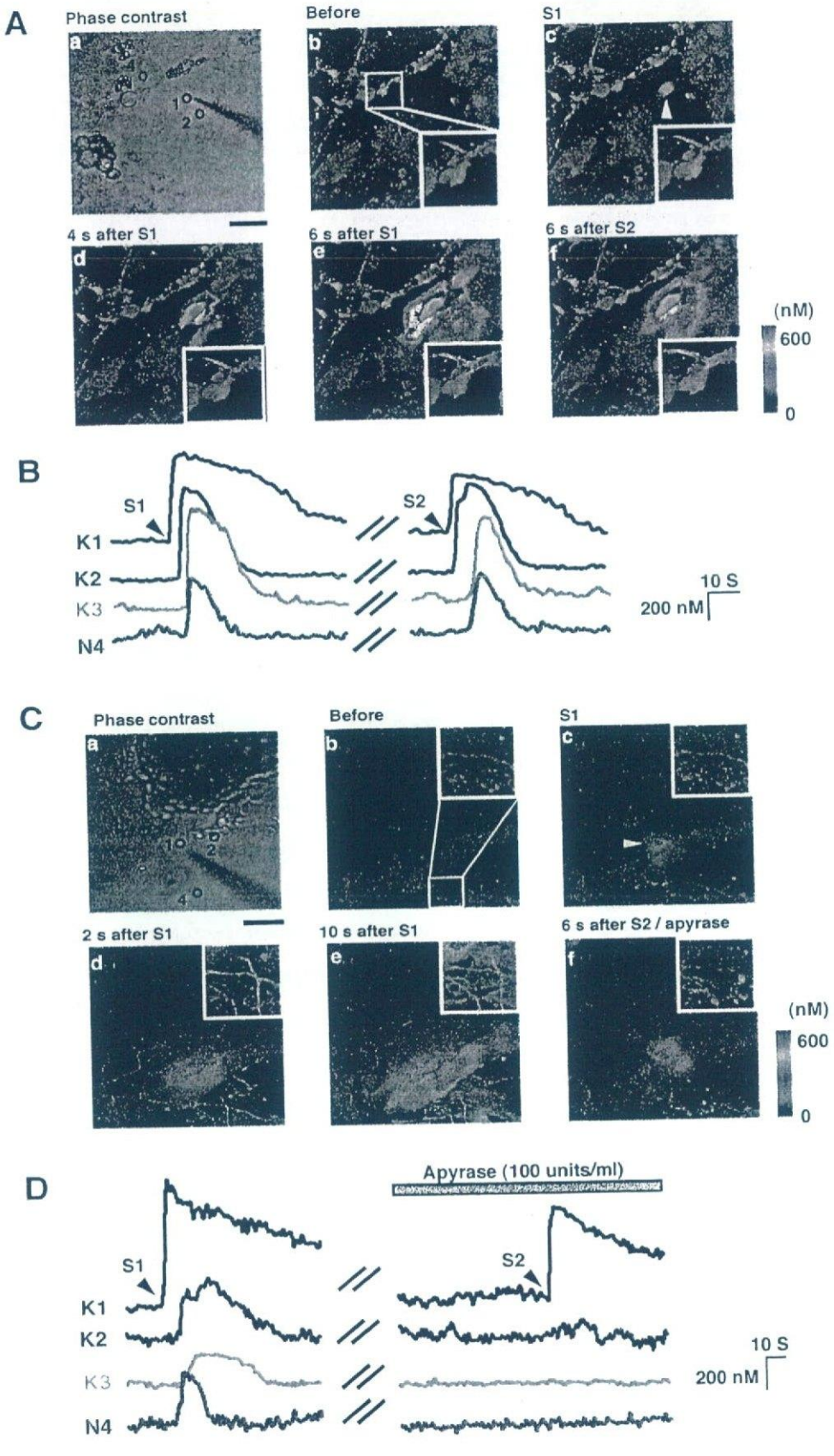

Figure 6 For legend see next page

followed by an increase in $[Ca^{2+}]_i$ in the DRG neurons after a time lag (Figures 6Ae and 6B, trace N4). The increases in $[Ca^{2+}]_i$ in DRG neurons were also dependent on extracellular ATP and the activation of P2 receptors, since the ATP-degrading enzyme, apyrase (grade III, 100 units/ml; Figures 6Cf and 6D), and suramin (100 μM) inhibited the increase in $[Ca^{2+}]_i$ (apyrase, $9.6 \pm 0.9\%$ of S1, $n = 21$; suramin, $14.8 \pm 1.9\%$ of S1, $n = 33$). Thus we concluded that the release of ATP in response to mechanical stimulation from NHEKs functions as an intercellular molecule between NHEKs and DRG neurons, which may affect nociceptive transduction in peripherin-positive neurons.

DISCUSSION

In the present study, we have demonstrated that ATP is a dominant extracellular signalling molecule in the formation of intercellular Ca^{2+} waves in NHEKs. We also showed that extracellular ATP-dependent Ca^{2+} waves in NHEKs caused increases in $[Ca^{2+}]_i$ in the adjacent DRG neurons. Thus ATP derived from NHEKs functions in both an autocrine and paracrine manner in the peripheral skin-to-sensory neuron system.

Both ATP and UTP caused increases in $[Ca^{2+}]_i$ in NHEKs to a similar extent. These Ca^{2+} responses were independent of extracellular Ca^{2+}, but dependent on inositol 1,4,5-trisphosphate-sensitive Ca^{2+} stores, suggesting the involvement of metabotropic P2Y receptors in the responses. ATP and UTP are natural ligands at $P2Y_2$ receptors, and are approximately equipotent. UTP also activates $P2Y_4$ receptors, but the human $P2Y_4$ receptor is highly selective for UTP than ATP [25]. UDP, an agonist to $P2Y_6$ receptors, only slightly increased the $[Ca^{2+}]_i$ in NHEKs [26,27]. Suramin moderately antagonizes human $P2Y_2$ receptors but not human $P2Y_4$ receptors [28]. NHEKs expressed a large amount of mRNAs for $P2Y_2$ receptors, but not for $P2Y_4$ or $P2Y_6$ receptors. All these pharmacological profiles showed that these responses should be mediated by $P2Y_2$ receptors (Figure 2). Very recently, Greig et al. [29] have reported that skin cells express P2X5, P2X7, $P2Y_1$ and $P2Y_2$ receptors, each of which is expressed in a spatially distinct zone of the epidermis and has distinct cellular functions. $P2Y_2$ receptors are expressed in the lower layer of the epidermis and are involved in proliferation, suggesting that the NHEKs used in the present study might mimic the basal cellular layer of skin cells *in vivo*.

The question remains as to whether endogenous ATP may produce propagating Ca^{2+} waves in NHEKs. Several reports have shown that mechanical stimulation produces a propagating Ca^{2+} wave in non-excitable cells such as astrocytes [15,30] and hepatocytes [12]. In astrocytes, extracellular molecules such as glutamate [11,31] and ATP [15,30], rather than gap junctions [32], are responsible for the propagation of Ca^{2+} waves. We sought to determine whether extracellular ATP produces intercellular Ca^{2+} waves in NHEKs. Mechanical stimulation of a single NHEK resulted in the induction of an intercellular Ca^{2+} wave, which was inhibited by the ATP-degrading enzyme, apyrase, and the P2 receptor antagonist, suramin (Figure 3). The gap junction inhibitor, 1-octanol, had little effect on the Ca^{2+} wave. Imaging of the ATP release by the modified luciferin–luciferase chemiluminescence clearly showed that the levels of extracellular ATP after mechanical stimulation were highest at the site of stimulation and decreased concentrically. These results strongly suggest that the mechanically evoked Ca^{2+} waves in NHEKs are mediated by extracellular ATP and by the activation of $P2Y_2$ receptors. As in astrocytes [15,30], extracellular ATP appears to play a pivotal role in creating the dynamic changes for long-range signalling in NHEKs.

The responses mediated by $P2Y_2$ receptors are probably layer-specific. The ATP-evoked hyperpolarization is very high in the basal layer but extremely low in the suprabasal layer in HaCaT keratinocytes [33]. The mRNA level of $P2Y_2$ receptors is down-regulated in differentiating HaCaT cells [34]. Thus the intercellular Ca^{2+} waves seen in the present study may be a response restricted to the basal layer of keratinocytes *in situ*. The finding that the barrier recovery rate of the mouse epidermis is regulated by functional P2 × 3 [35] suggests that the skin expresses multiple P2 receptors that are linked to distinct physiological functions.

There is an increasing body of evidence that ATP, the predominant extracellular signalling molecule of astrocytes [15,30], may also mediate signalling between neurons and glial cells [36–38]. With regard to the skin-to-sensory neuron system, a similar relationship may also be obtained. Especially, non-myelinated small-sized DRG neurons (nociceptors) terminate in the periphery as free nerve endings [39]. Thus nociceptors can directly contact skin-derived extracellular molecules when skin cells are injured, inflamed or otherwise stimulated. When cells are injured or destroyed, very high concentrations of intracellular ATP (> 5 mM) could leak and affect the surrounding NHEKs and DRG neurons. In the present study, however, we showed that the intercellular Ca^{2+} waves in NHEKs were reproducible when the same cell was stimulated repeatedly (Figure 6). Moreover, the increases in neuronal $[Ca^{2+}]_i$ in response to mechanical stimulation of NHEKs were also reproducible. Thus it appears that extracellular ATP-mediated NHEK-to-DRG neuron communication takes place even when cell damage is not involved. Somatic sensation requires the conversion of physical stimuli into depolarization of the distal nerve endings. It has been reported that activation of $P2Y_1$ receptors in sensory fibres increases the frequency of spikes evoked by a light touch of the skin [40]. Therefore the skin might sense and transmit non-harmful stimuli to sensory neurons via ATP.

DRG neurons express various types of P2 receptors. Ionotropic P2X receptors, especially P2X3 [41] and P2X2 [42] receptors in small- and middle-sized DRG neurons respectively, have been extensively studied in relation to pain. However, recent reports suggest that some P2Y receptors are present in small-sized DRG neurons and are involved in pain signalling. In small-sized neurons, activation of $P2Y_1$ or $P2Y_2$ receptors sensitizes TRPV1 receptors via protein kinase C-dependent mechanisms [43], stimulation of $P2Y_2$ receptors enhances the $[Ca^{2+}]$ increase, leading to the release of CGRP [44], and activation of $P2Y_2$

Figure 6 Dynamic communication between NHEKs and DRG neurons mediated by extracellular ATP

(**A**) Phase-contrast image (**a**) and pseudo colour $[Ca^{2+}]_i$ images (self-ratios of fluo-4 fluorescence; **b–f**) in co-cultured NHEKs and DRG neurons obtained by confocal laser microscopy. The white rectangle field in the middle of image **b** is shown enlarged in the bottom right of images **b–f**. The red arrowhead in image **b** depicts position 4 (DRG neuron 4). The white arrowhead in image **c** shows the initiation of Ca^{2+} wave in response to mechanical stimulation (cell 1). Scale bar, 50 μm. (**B**) The graph shows individual traces of the self-ratios of fluo-4 fluorescence in keratinocytes (K1–K3) and DRG neuron (N4) shown in image **Aa**. Keratinocyte 1 was mechanically stimulated twice (arrows S1 and S2) separated by 5 min. (**C**) Phase-contrast image (**a**) and pseudo colour $[Ca^{2+}]_i$ images (self-ratios of fluo-4 fluorescence; **b–f**) in co-cultured NHEKs and DRG neurons. The white rectangle field in the middle of image **b** is shown enlarged in the top right of images **b–f**. The red arrowhead in image **b** depicts position 4 (DRG neuron 4). The white arrowhead in image **c** shows the initiation of Ca^{2+} wave in response to mechanical stimulation (cell 1). Scale bar, 50 μm. (**D**) The graph shows individual traces of self-ratios of fluo-4 fluorescence in keratinocytes (K1–K3) and DRG neuron (N4) shown in image **a** in **C**. Keratinocyte 1 was mechanically stimulated twice (arrows S1 and S2) separated by 5 min. The first and second mechanical stimulations were performed in the absence and presence of 100 units/ml apyrase (grey horizontal bar).

receptors results in phosphorylation of CREB (cAMP-response-element-binding protein) [45]. We showed that approx. 70% of both small-sized DRG neurons and NHEKs possess functional $P2Y_2$ receptors in the co-culture (Figure 5). In the peripheral skin-to-sensory neuron system, $P2Y_2$ receptors might be the main sensor for both NHEKs and DRG neurons. However, we cannot exclude the possibility that Ca^{2+} entry via P2X receptors is also involved in Ca^{2+} signalling in DRG neurons. In fact, when skin cells are killed, a large amount of intracellular ATP in the skin leaks and excites nociceptors by activating P2X receptors [46]. In a skin–nerve preparation, carrageenan inflammation of skin resulted in an increase in the activities of c-fibres, which was mediated by P2X receptors [47]. There might be multiple mechanisms by which the skin communicates with sensory neurons through ATP.

Apart from those of cell injury, the mechanisms underlying ATP release from NHEKs remain unknown. In neuronal cells, depolarizing stimulation resulted in exocytotic release of ATP in hippocampal slices [48] and cultured hippocampal neurons [49]. However, in non-excitable cells including NHEKs, the mechanism of ATP release is still a matter of debate. In astrocytes, there have been several reports that ATP can be released via chloride channels [50], gap junction hemi-channels [51], ATP-binding cassette [52] and exocytosis [53,54]. NHEKs also express several types of chloride channels [34,55,56], connexins [57–59] and SNARE (soluble *N*-ethylmaleimide-sensitive fusion protein attachment protein receptor) proteins [60,61]. Although these similarities raise the possibility that NHEKs and astrocytes might share the same mechanism for the release of ATP, further investigation is needed.

In summary, we demonstrated that extracellular ATP derived from NHEKs functions in both an autocrine and paracrine manner in the peripheral skin-to-sensory neurons system. Metabotropic $P2Y_2$ receptors may be important sensors for extracellular ATP in both NHEKs and small-sized DRG neurons.

We thank T. Obama (Division of Biosignaling, National Institute of Health Sciences) for helping in the culturing of cells and Y. Ohno (Division of Pharmacology, National Institute of Health Sciences) for continuous encouragement. This work was partially supported by the Organization for Pharmaceutical Safety and Research (Medical Frontier Project; MF-16), the Health Science Foundation (Japan) and Shiseido Research Center (Yokohama, Japan).

REFERENCES

1 Denda, M., Fuziwara, S., Inoue, K., Denda, S., Akamatsu, H., Tomitaka, A. and Matsunaga, K. (2001) Immunoreactivity of VR1 on epidermal keratinocyte of human skin. Biochem. Biophys. Res. Commun. **285**, 1250–1252

2 Inoue, K., Koizumi, S., Fuziwara, S., Denda, S. and Denda, M. (2002) Functional vanilloid receptors in cultured normal human epidermal keratinocytes. Biochem. Biophys. Res. Commun. **291**, 124–129

3 Grando, S. A. (1997) Biological functions of keratinocyte cholinergic receptors. J. Investig. Dermatol. Symp. Proc. **2**, 41–48

4 Arredondo, J., Nguyen, V. T., Chernyavsky, A. I., Bercovich, D., Orr-Urtreger, A., Kummer, W., Lips, K., Vetter, D. E. and Grando, S. A. (2002) Central role of α7 nicotinic receptor in differentiation of the stratified squamous epithelium. J. Cell Biol. **159**, 325–336

5 Genever, P. G., Maxfield, S. J., Kennovin, G. D., Maltman, J., Bowgen, C. J., Raxworthy, M. J. and Skerry, T. M. (1999) Evidence for a novel glutamate-mediated signaling pathway in keratinocytes. J. Invest. Dermatol. **112**, 337–342

6 Dixon, C. J., Bowler, W. B., Littlewood-Evans, A., Dillon, J. P., Bilbe, G., Sharpe, G. R. and Gallagher, J. A. (1999) Regulation of epidermal homeostasis through P2Y2 receptors. Br. J. Pharmacol. **127**, 1680–1686

7 Stoebner, P. E., Carayon, P., Penarier, G., Frechin, N., Barneon, G., Casellas, P., Cano, J. P., Meynadier, J. and Meunier, L. (1999) The expression of peripheral benzodiazepine receptors in human skin: the relationship with epidermal cell differentiation. Br. J. Dermatol. **140**, 1010–1016

8 Zia, S., Ndoye, A., Lee, T. X., Webber, R. J. and Grando, S. A. (2000) Receptor-mediated inhibition of keratinocyte migration by nicotine involves modulations of calcium influx and intracellular concentration. J. Pharmacol. Exp. Ther. **293**, 973–981

9 Wall, F. M., Hudson, D. L., Lamb, A. G., Bolsover, S. R., Silver, R. A., Aitchison, M. J. and Whitaker, M. (1991) Mitogens induce calcium transients in both dividing and terminally differentiating keratinocytes. J. Cell Sci. **99**, 397–405

10 Cornell-Bell, A. H., Finkbeiner, S. M., Cooper, M. S. and Smith, S. J. (1990) Glutamate induces calcium waves in cultured astrocytes: long-range glial signaling. Science **247**, 470–473

11 Charles, A. C., Merrill, J. E., Dirksen, E. R. and Sanderson, M. J. (1991) Intercellular signaling in glial cells: calcium waves and oscillations in response to mechanical stimulation and glutamate. Neuron **6**, 983–992

12 Thomas, A. P., Renard, D. C. and Rooney, T. A. (1991) Spatial and temporal organization of calcium signalling in hepatocytes. Cell Calcium **12**, 111–126

13 Hansen, M., Boitano, S., Dirksen, E. R. and Sanderson, M. J. (1993) Intercellular calcium signaling induced by extracellular adenosine 5′-triphosphate and mechanical stimulation in airway epithelial cells. J. Cell Sci. **106**, 995–1004

14 Demer, L. L., Wortham, C. M., Dirksen, E. R. and Sanderson, M. J. (1993) Mechanical stimulation induces intercellular calcium signaling in bovine aortic endothelial cells. Am. J. Physiol. **264**, H2094–H2102

15 Guthrie, P. B., Knappenberger, J., Segal, M., Bennett, M. V., Charles, A. C. and Kater, S. B. (1999) ATP released from astrocytes mediates glial calcium waves. J. Neurosci. **19**, 520–528

16 Scemes, E., Dermietzel, R. and Spray, D. C. (1998) Calcium waves between astrocytes from Cx43 knockout mice. Glia **24**, 65–73

17 Cauna, N. (1973) The free penicillate nerve endings of the human hairy skin. J. Anat. **115**, 277–288

18 Hilliges, M., Wang, L. and Johansson, O. (1995) Ultrastructural evidence for nerve fibers within all vital layers of the human epidermis. J. Invest. Dermatol. **104**, 134–137

19 Peier, A. M., Reeve, A. J., Andersson, D. A., Moqrich, A., Earley, T. J., Hergarden, A. C., Story, G. M., Colley, S., Hogenesch, J. B., McIntyre, P. et al. (2002) A heat-sensitive TRP channel expressed in keratinocytes. Science **296**, 2046–2049

20 Hensel, H. and Iggo, A. (1971) Analysis of cutaneous warm and cold fibres in primates. Pflugers Arch. **329**, 1–8

21 Hensel, H. and Kenshalo, D. R. (1969) Warm receptors in the nasal region of cats. J. Physiol. (Cambridge, U.K.) **204**, 99–112

22 Grynkiewicz, G., Poenie, M. and Tsien, R. Y. (1985) A new generation of Ca^{2+} indicators with greatly improved fluorescence properties. J. Biol. Chem. **260**, 3440–3450

23 Koizumi, S., Rosa, P., Willars, G. B., Challiss, R. A., Taverna, E., Francolini, M., Bootman, M. D., Lipp, P., Inoue, K., Roder, J. et al. (2002) Mechanisms underlying the neuronal calcium sensor-1-evoked enhancement of exocytosis in PC12 cells. J. Biol. Chem. **277**, 30315–30324

24 Koizumi, S., Bootman, M. D., Bobanovic, L. K., Schell, M. J., Berridge, M. J. and Lipp, P. (1999) Characterization of elementary Ca^{2+} release signals in NGF-differentiated PC12 cells and hippocampal neurons. Neuron **22**, 125–137

25 Communi, D., Pirotton, S., Parmentier, M. and Boeynaems, J. M. (1995) Cloning and functional expression of a human uridine nucleotide receptor. J. Biol. Chem. **270**, 30849–30852

26 Chang, K., Hanaoka, K., Kumada, M. and Takuwa, Y. (1995) Molecular cloning and functional analysis of a novel P2 nucleotide receptor. J. Biol. Chem. **270**, 26152–26158

27 Communi, D., Parmentier, M. and Boeynaems, J. M. (1996) Cloning, functional expression and tissue distribution of the human P2Y6 receptor. Biochem. Biophys. Res. Commun. **222**, 303–308

28 Communi, D., Motte, S., Boeynaems, J. M. and Pirotton, S. (1996) Pharmacological characterization of the human P2Y4 receptor. Eur. J. Pharmacol. **317**, 383–389

29 Greig, A. V., Linge, C., Terenghi, G., McGrouther, D. A. and Burnstock, G. (2003) Purinergic receptors are part of functional signaling system for proliferation and differentiation of human epidermis keratinocytes. J. Invest. Dermatol. **120**, 1007–1015

30 Fam, S. R., Gallagher, C. J. and Salter, M. W. (2000) P2Y1 purinoceptor-mediated Ca^{2+} signaling and Ca^{2+} wave propagation in dorsal spinal cord astrocytes. J. Neurosci. **20**, 2800–2808

31 Newman, E. A. and Zahs, K. R. (1998) Modulation of neuronal activity by glial cells in the retina. J. Neurosci. **18**, 4022–4028

32 Finkbeiner, S. (1992) Calcium waves in astrocytes – filling in the gaps. Neuron **8**, 1101–1108

33 Burgstahler, R., Koegel, H., Rucker, F., Tracey, D., Grafe, P. and Alzheimer, C. (2003) Confocal ratiometric voltage imaging of cultured human keratinocytes reveals layer-specific responses to ATP. Am. J. Physiol. **284**, C944–C952

34 Koegel, H. and Alzheimer, C. (2001) Expression and biological significance of Ca^{2+}-activated ion channels in human keratinocytes. FASEB J. **15**, 145–154